JOURNAL OF VIROLOGY, Jan. 2003, p. 600–623 Vol. 77, No. 1
0022-538X/03/$08.00+0 DOI: 10.1128/JVI.77.1.600–623.2003

Role of CCAAT/Enhancer-Binding Protein Alpha (C/EBPα) in Activation of the Kaposi's Sarcoma-Associated Herpesvirus (KSHV) Lytic-Cycle Replication-Associated Protein (RAP) Promoter in Cooperation with the KSHV Replication and Transcription Activator (RTA) and RAP

Shizhen Emily Wang,[1] Frederick Y. Wu,[1,2] Masahiro Fujimuro,[1] Jianchao Zong,[1] S. Diane Hayward,[1,2] and Gary S. Hayward[1,2]*

Molecular Virology Laboratories, Department of Pharmacology and Molecular Sciences,[2] and Viral Oncology Program, Sidney Kimmel Comprehensive Cancer Center,[1] School of Medicine, The Johns Hopkins University, Baltimore, Maryland 21231-1000

Received 28 June 2002/Accepted 20 September 2002

The Kaposi's sarcoma-associated herpesvirus (KSHV)-encoded replication-associated protein (RAP, or K8) has been shown to induce both CCAAT/enhancer binding protein alpha (C/EBPα) and $p21^{CIP-1}$ expression, resulting in G_0/G_1 cell cycle arrest during the lytic cycle. RAP and C/EBPα are also known to interact strongly both in vitro and in lytically infected cells. We recognized two potential consensus C/EBP binding sites in the RAP promoter and performed electrophoretic mobility shift assay (EMSA) analysis with in vitro-translated C/EBPα; this analysis showed that one of these sites has a very high affinity for C/EBPα. Luciferase (LUC) assays performed with a target RAP promoter-LUC reporter gene confirmed that C/EBPα can transcriptionally activate the RAP promoter up to 50-fold. Although RAP had no effect on its own promoter by itself, the addition of RAP and C/EBPα together resulted in a threefold increase in activity over that obtained with C/EBPα alone. Importantly, the introduction of exogenous Flag-tagged C/EBPα triggered RAP expression in BCBL-1 cells latently infected with KSHV, as detected by both reverse transcription-PCR and double-label immunofluorescence assay analyses, suggesting the presence of a self-reinforcing loop with C/EBPα and RAP activating each other. The RAP promoter can also be activated 50- to 120-fold by the KSHV lytic-cycle-triggering protein known as replication and transcription activator (RTA). C/EBPα and RTA together cooperated to elevate RAP promoter activity four- to sixfold more than either alone. Furthermore, the addition of RAP, C/EBPα, and RTA in LUC reporter cotransfection assays resulted in 7- to 15-fold more activation than that seen with either C/EBPα or RTA alone. Site-specific mutational analysis of the RAP promoter showed that the strong C/EBP binding site is crucial for C/EBPα-mediated transactivation of the RAP promoter. However, the C/EBP binding site also overlaps the previously reported 16-bp RTA-responsive element (RRE), and the same mutation also both reduced RTA-mediated transactivation and abolished the cooperativity between C/EBPα and RTA. Furthermore, in vitro-translated RTA, although capable of binding directly to the polyadenylated nuclear RNA (PAN) RRE motif, failed to bind to the RAP RRE and interfered with RRE-bound C/EBPα in EMSA experiments. Partial RTA responsiveness but no cooperativity could be transferred to a heterologous promoter containing added consensus C/EBP binding sites. A chromatin immunoprecipitation assay showed that all three proteins associated specifically with RAP promoter DNA in vivo and that, when C/EBPα was removed from a tetradecanoyl phorbol acetate-treated JSC-1 primary effusion lymphoma cell lysate, the levels of association of RTA and RAP with the RAP promoter were reduced 3- and 13-fold, respectively. Finally, RTA also proved to physically interact with both C/EBPα and RAP, as assayed both in vitro and by immunoprecipitation. Binding to C/EBPα occurred within the N-terminal DNA binding domain of RTA, and deletion of a 17-amino-acid basic motif of RTA abolished both the C/EBPα and DNA binding activities as well as all RTA transactivation and the cooperativity with C/EBPα. Therefore, we suggest that RTA transactivation of the RAP RRE is mediated by an interaction with DNA-bound C/EBPα but that full activity requires more than just the core C/EBP binding site.

Kaposi's sarcoma (KS)-associated herpesvirus (KSHV) is a gamma-2-class herpesvirus that is related to Epstein-Barr virus (EBV) but contains several novel loci (5, 6, 29, 34). KSHV DNA and latency-associated nuclear antigen 1 (LANA1) are present in virtually all tumor samples of classical endemic and AIDS-associated forms of KS (6) as well as in peripheral blood mononuclear cells of up to 50% of homosexual AIDS patients with KS (48); seropositivity is rare in healthy blood donors. KSHV is also present in a limited subset of AIDS-associated lymphoproliferative disorders referred to as primary effusion lymphomas (PELs) and multicentric Castleman's disease (3, 4, 37). PEL cell lines are B-cell lymphoma cells that are latently infected with KSHV, that carry multicopy KSHV episomes, and that can be induced into the lytic cycle by treatment with

* Corresponding author. Mailing address: CRB-3M08, 1650 Orleans St., Baltimore, MD 21231-1000. Phone: (410) 955-8684. Fax: (410) 955-8685. E-mail: ghayward@jhmi.edu.

tetradecanoyl phorbol acetate (TPA) or sodium butyrate (4, 33). KSHV can also infect human primary dermal microvascular endothelial cells and converts them to LANA1-positive spindle-shaped cells that are morphologically similar to the characteristic spindle-shaped cells of nodular KS lesions (3, 11).

Like EBV, KSHV undergoes two distinct phases of infection, namely, latency and a reactivated productive lytic cycle, and the expression patterns for latent genes and lytic genes are mutually exclusive. During KSHV latency, only a small number of oncogenic and antiapoptotic viral genes encoded by KSHV, such as those for LANA1, v-FLIP, v-CycD, and K15/LAMP, are expressed; the rest of the genome is silent (5, 29, 34). Although the KSHV lytic cycle is not directly associated with neoplastic transformation, it is required for the release of infectious particles and the spread of KSHV infections. During reactivation in vivo, higher loads of virus are detected in the systemic circulation as a result of efficient viral lytic gene expression and viral DNA replication.

The KSHV-encoded replication-associated protein (RAP, or K8) is a 237-amino-acid early nuclear protein that is expressed in the lytic cycle and that is evolutionarily distantly related to the EBV lytic-cycle Z transactivator (ZTA) protein. Unlike ZTA, RAP is unable to trigger the viral lytic cycle on its own (26, 32) and is not known to bind to DNA or to function as a direct transcriptional activator (24, 50). Like ZTA, RAP contains a leucine zipper oligomerization domain and may interact with p53 and CBP (18, 31), but it is not known whether RAP can modulate expression from its own promoter. However, RAP evidently plays an important role in KSHV DNA replication because it is efficiently recruited into viral DNA replication compartments both when assembled in vitro in DNA-transfected Vero cells and when formed in vivo during the lytic cycle in KSHV-infected PEL or endothelial cells, as detected by immunofluorescence assay (IFA) studies (50).

During the early stages of the KSHV lytic cycle, RAP is induced approximately 12 h after the initiation of KSHV lytic-cycle replication, and its expression is maintained throughout the lytic cycle (24, 52). When first synthesized, RAP also is targeted to small subnuclear punctate bodies known as PML oncogenic domains (PODs); however, unlike the situation with several other herpesvirus POD-targeting proteins, this targeting does not result in the loss of PML protein from the PODs (50). Recent studies have reported that the immediate-early KSHV replication and transcription activator (RTA, or ORF50), a nuclear protein, is an upstream transcriptional activator of the RAP promoter (16, 25–27, 45). KSHV RTA, a homologue of EBV RTA, is induced within 4 h after lytic-cycle initiation (38) and is capable of inducing the full lytic cycle of KSHV when introduced into latently infected cells (16, 26, 27). After mapping of the RAP promoter through exhaustive linker-scanning mutagenesis, RTA was reported to mediate transcriptional activation of the RAP promoter through an RTA-responsive element (RRE) containing a 16-bp consensus sequence (5′-74769-GTGAAACAATAATGAT-74785-3′); deletion of this 16-bp sequence resulted in a significant loss of RTA responsiveness in all cell types tested (25, 45). Lukac et al. (25) later reported that KSHV RTA is able to bind to this DNA sequence on the RAP promoter directly to activate RAP expression. However, the possibility that cellular transcription factors may also be involved has not yet been evaluated.

It was recently found that KSHV RAP mediates G_1 cell cycle arrest through induction of the cellular proteins CCAAT/enhancer binding protein alpha (C/EBPα) and p21 (49, 50a). C/EBPs (C/EBPα, C/EBPβ, and CHOP-10) belong to the bZIP family of nuclear transcription factors, including also c-JUN, c-FOS, CREB, and ZTA (19), and C/EBPα plays important roles as the determining factor for adipocyte, granulocyte, and neutrophil differentiation (13, 20, 47, 51). The C/EBPα gene encodes two predominant isoforms, namely, a 42-kDa full-length form that has antimitotic activity and a 30-kDa truncated form that is made from an alternative translation initiation site and that lacks antimitotic activity (2, 23, 30). C/EBPα can positively autoregulate its own gene promoter (10, 39, 40) and controls differentiation and G_1 cell cycle arrest through three reported mechanisms: (i) up-regulation of the expression of the cdk2, cdk4, and cdk6 inhibitor $p21^{CIP}$ (41, 42); (ii) inhibition of E2F transcription (35); and (iii) direct inhibition of cdk2 and cdk4 (17, 44).

Evidence is accumulating that herpesvirus DNA replication takes place only in G_1-arrested host cells, possibly to prevent competition with host cell DNA synthesis for limited free nucleotides and to provide nuclear spaces for progeny viral DNA accumulation (15). In KSHV-infected cells, C/EBPα expression is induced either during lytic-cycle induction by TPA or by direct introduction of exogenous KSHV RAP, leading to host cell cycle arrest at G_1 (49). Importantly, it has also been found that RAP binds strongly to C/EBPα both in vitro in glutathione *S*-transferase (GST) affinity assay and electrophoretic mobility shift assay (EMSA) experiments and in lytically infected cells, as detected by immunoprecipitation and colocalization experiments. Furthermore, RAP enhances C/EBPα expression through transcriptional synergy with C/EBPα and possibly also through C/EBPα stabilization (F. Y. Wu, Q. Tang, S. E. Wang, M. Fujimuro, C.-J. Chiou, S. D. Hayward, M. D. Lane, and G. Hayward, unpublished data).

In the present study, we found a strong C/EBP binding site in the RAP promoter which overlaps the known RRE. Therefore, we evaluated how C/EBPα affects the activation of the KSHV RAP promoter both alone and in combination with RTA and RAP. Indeed, C/EBPα was able to strongly activate the RAP promoter in transient reporter gene assays and also activated RAP expression after introduction into PEL cells. Furthermore, cotransfected KSHV RTA and C/EBPα cooperatively enhanced the transcriptional activation of a target KSHV RAP promoter-LUC reporter. We also found that C/EBPα and RAP both physically interacted with KSHV-encoded RTA. We suggest that RTA activation of the RAP promoter is partially mediated by C/EBPα and that either C/EBPα or RTA can trigger RAP expression, with RTA, C/EBPα, and RAP later acting in synergy to produce rapid high-level expression of RAP at the early stages of the lytic cycle.

MATERIALS AND METHODS

Cells and plasmids. KSHV-positive human PEL cell lines BCBL-1 and JSC-1 as well as KSHV-negative cell line DG75 were grown in RPMI 1640 medium (Invitrogen, Carlsbad, Calif.) containing 10% fetal bovine serum in a humidified 5% CO_2 incubator at 37°C. For KSHV lytic-cycle induction, TPA was added to

the medium at a final concentration of 20 ng/ml. Vero cells and HeLa cells were grown in Dulbecco's modified Eagle's medium (Invitrogen) containing 10% fetal bovine serum.

Plasmid pSEW-C01 is a full-length C/EBPα(1–358) mammalian expression plasmid in the pcDNA3.1 vector (Invitrogen) background driven by the human cytomegalovirus enhancer-promoter region, and plasmid pSEW-C02, based on the pCMV-Tag2 vector (Stratagene, La Jolla, Calif.), expresses full-length Flag-tagged C/EBPα(1–358). Plasmid pSEW-C05 encodes the full-length GST-C/EBPα(1–358) fusion. Plasmid pYNC172a (7) is a black beetle virus leader region (BBV)-enhanced T7 in vitro translation vector encoding full-length C/EBPα(1–358). Expression plasmid pJX15, encoding full-length KSHV RTA(1–691), was used to construct the following RTA deletion derivatives: pSEW-R02 encoding RTA(1–548); pSEW-R03 encoding RTA(1–377); pSEW-R04 encoding RTA(1–273); pSEW-R05 encoding RTA(273–691); pSEW-R06 encoding RTA(151–548); pSEW-R07 encoding RTA(210–548); pSEW-R08 encoding RTA(244–548); pSEW-R09 encoding RTA(1–377Δ11–67), with an in-frame internal deletion from positions 11 to 67; pSEW-R10 encoding RTA(1–377Δ11–112), with an in-frame internal deletion from positions 11 to 112; pSEW-R11 encoding RTA(1–691Δ11–272), with an in-frame internal deletion from positions 11 to 272; and pSEW-R23 encoding RTA(1–691Δ151–167), with an in-frame internal deletion from positions 151 to 167.

From the parent plasmid pSEW-R06 encoding RTA(151–548), additional amino acid mutations were introduced by PCR-based site-directed mutagenesis to generate pSEW-R12 encoding RTA(151–548K) (Lys at positions 152 and 154 is replaced by Glu), pSEW-R13 encoding RTA(151–548R1) (Arg at positions 160 and 161 is replaced by Glu and Gly, respectively), pSEW-R14 encoding RTA(151–548R2) (Arg at positions 166 and 167 is replaced by Gly and Glu, respectively), pSEW-R15 encoding RTA(151–548KR1) (combining substitutions K152E, K154E, R160E, and R161G), pSEW-R16 encoding RTA(151–548KR2) (combining substitutions R160E, R161G, R166G, and R167E), pSEW-R17 encoding RTA(151–548RR) (combining substitutions K152E, K154E, R166G, and R167E), and pSEW-R18 encoding RTA(151–548KRR) (combining all six substitutions). Plasmids encoding Flag-tagged, c-Myc-tagged, and GST fusion versions of full-length RTA(1–691) were designated pJX16 (pSEW-R19), pSEW-c-Myc-RFL (pSEW-R20), and pFYW39 (pSEW-R21), respectively. The GST-RTA(1–377) DNA binding domain (DBD) fusion (derived from pFYW39) was designated pFYW40 (pSEW-R22). Plasmid pFYW01 encodes intact c-Myc-tagged RAP(1–236) (50), and pCJC514 encodes BBV RAP, used for enhanced in vitro translation of intact RAP(1–236) (Wu et al., unpublished).

Plasmid pFYW41 (pSEW-P01) (pGL3-Basic background) contains the RAP(−190/+10)-LUC reporter gene driven by the RAP promoter region (positions −190 and +10) between coordinates 74655 and 74854 of the KSHV (BC1) genome (GenBank accession no. U75698). Plasmid pSEW-P10 contains the PAN-LUC reporter gene driven by a 220-bp polyadenylated nuclear RNA (PAN) promoter region. Additional deletion derivatives of the target RAP-LUC reporter gene were generated by PCR-based site-directed mutagenesis with pFYW41 as the template to create RAP-(PM1)-LUC, with TGT at positions −87 to −85 replaced by ATC to create an *Eco*RV site (pSEW-P02); RAP-(PM2)-LUC, with ACA at positions −71 to −69 replaced by TTC to create an *Eco*RI site (pSEW-P03); and RAP-(PM1 + 2)-LUC, with both mutations (pSEW-P04). Two additional heterologous LUC reporter genes in the A10 minimal simian virus 40 T-antigen promoter (−150/+50) background were generated: $(\text{RAP-C/EBP-II})_3$-A10-LUC (in plasmid pSEW-P05), which contains three tandem copies of a 20-bp oligonucleotide encompassing the core C/EBP-II motif (AAACAAT) found in the KSHV RAP promoter, and $(\text{C/EBP-wt})_3$-A10-LUC (in plasmid pSEW-P06), which contains three tandem copies of a 20-bp oligonucleotide encompassing the wild-type palindromic consensus C/EBP binding site (ATTGCGCAAT) (43).

DNA transfection and LUC assay. BCBL-1 and DG75 cells were transfected by the electroporation method described previously (46). First, 10^7 cells were mixed with 5 to 10 μg of plasmid DNA in 0.5 ml of RPMI 1640 medium and electroporated at 300 V and 950 μF by using a GenePulser (Bio-Rad, Hercules, Calif.). Transfections of Vero and HeLa cells were performed with Lipofectamine (Invitrogen) according to the manufacturer's protocol. Cells were seeded at 5×10^5 per well in six-well plates 1 day prior to transfection. Cells were transfected with a total amount of 1.5 to 2.5 μg of DNA and harvested at 48 h posttransfection. LUC activity was measured for 10 s with a Lumat LB9501 luminometer (Berthold Systems, Inc.) by using a LUC assay system (Promega, Madison, Wis.).

Extraction of mRNA and RT-PCR. BCBL-1 cells were transfected by electroporation, and mRNA was extracted at 40 h posttransfection by using a GenElute Direct mRNA miniprep kit (Sigma, St. Louis, Mo.) according to the product instructions. Cells were harvested and resuspended by vortexing in 0.5 ml of a lysis solution containing proteinase K (0.2 mg/ml), followed by incubation at 65°C for 10 min. Then, 32 μl of 5 M NaCl and 25 μl of oligo(dT) beads were added to the solution and allowed to stand at room temperature for 10 min. The oligo(dT)-mRNA complexes were pelleted by centrifugation for 5 min at 10,000 × *g*, washed once in 350 μl of wash solution, and washed twice in 350 μl of low-salt wash solution. The poly(A) mRNA was eluted at 65°C in 100 μl of elution solution. For reverse transcription (RT), the following reagents were mixed and incubated at 42°C for 1 h: 20 U of avian myeloblastosis virus reverse transcriptase (Promega), 10 μl of avian myeloblastosis virus 5× RT buffer (Promega), 1 μl of rRNasin RNA inhibitor (Promega), 4 μl of 5 mM deoxynucleoside triphosphates (dNTPs), 0.5 μg of random primers (Promega), 30 μl of mRNA, and H_2O to a final volume of 50 μl. The synthesized cDNA samples were used as templates for PCRs with primers LGH3771 (5′-CGCGGATCCAATTTGAAGAGGAACGCTTA-3′) and LGH3774 (5′-CGCGGATCCTCAACATGGTGGGAGTGG-3′) in a mixture containing 2 μl of cDNA template, 0.25 μg of each primer, 3 μl of 25 mM $MgCl_2$, 4 μl of 2.5 mM dNTPs, 3.5 μl of dimethyl sulfoxide, 2.5 U of *Taq* DNA polymerase (Promega), 5 μl of thermophilic DNA polymerase 10× buffer (Promega), and H_2O to a final volume of 50 μl. The conditions for PCR were 1 cycle at 94°C for 5 min; 30 cycles at 94°C for 1 min, 55°C for 1 min, and 72°C for 1 min; and 1 cycle at 72°C for 10 min. The PCR products were analyzed on a 2% agarose gel.

EMSA. Proteins used in the EMSA were in vitro translated by using a TNT quick coupled transcription-translation system (Promega) according to the manufacturer's procedures. Mixtures containing 2 μg of plasmid DNA, 1 μl of RNase inhibitor, 2 μl of 1 mM "cold" methionine, and 40 μl of TNT Quick Master Mix were incubated at 30°C for 90 min and stored at −80°C. Correct protein expression was verified by adding 2 μl of [^{35}S]methionine (Amersham Pharmacia, Piscataway, N.J.) instead of nonradioactive methionine to the reaction mixtures, and the products were analyzed by sodium dodecyl sulfate (SDS)-polyacrylamide gel electrophoresis (PAGE) and autoradiography. For the EMSA, 2 to 4 μl of in vitro-translated proteins was used for each reaction in a binding system containing 10 mM HEPES (pH 7.5), 50 mM KCl, 1 mM EDTA, 1 mM dithiothreitol, 1 mM phenylmethylsulfonyl fluoride (PMSF), 1% Triton X-100, 5% glycerol, and 2 μg of poly(dI-dC). After annealing, double-stranded oligonucleotides were radiolabeled with [α-^{32}P]dCTP by incubation with Klenow DNA polymerase in the presence of dNTP (minus dCTP). Approximately 50,000 cpm of the ^{32}P-labeled probe was added to each sample and incubated for 30 min at room temperature. For competition assays, unlabeled oligonucleotides were added to the sample to compete for binding against the ^{32}P-labeled probe at a molar ratio of 100:1. For supershift experiments, 0.5 μl of C/EBPα or RTA antiserum was added to the mixture after 30 min and incubated for 30 min before gel loading. Samples were separated on a 4.5% polyacrylamide gel in a buffer containing 10 mM HEPES (pH 7.5), 1 mM EDTA, and 0.5 mM EGTA at 150 V and 4°C as described previously (8). The gel was subsequently dried and subjected to autoradiography with Kodak film.

All oligonucleotides used were purchased from Invitrogen and are listed below (mutated nucleotides are shown in bold type). LGH3973 (5′-GATCGGTTGATTGTGACTATTTGTGAAACAATAATGA-3′) and LGH3974 (5′-GATCTCATTATTGTTTCACAAATAGTCACAATCAACC-3′) were annealed to form probe RAP-PWT; LGH4262 (5′-GATCGGTTGAT**ATC**GACTATTTGTGAAACAATAATGA-3′) and LGH4263 (5′-GATCTCATTATTGTTTCACAAATAGTC**GAT**ATCAACC-3′) were annealed to form probe RAP-PM1; LGH4264 (5′-GATCGGTTGATTGTGACTATTTGTGAA**TTC**ATAATGA-3′) and LGH4265 (5′-GATCTCATTAT**GAA**TTCACAAATAGTCACAATCAACC-3′) were annealed to form probe RAP-PM2; LGH4266 (5′-GATCGGTTGAT**ATC**GACTATTTGTGAA**TTC**ATAATGA-3′) and LGH4267 (5′-GATCTCATTAT**GAA**TTCACAAATAGTC**GAT**ATCAACC-3′) were annealed to form probe RAP-PM1 + 2; LGH4268 (5′-GATCGATTGTGACTATTTGTGAAACAATAATGATTAAAGGGGGTGGTATTTCC-3′) and LGH4269 (5′-GATCGGAAATACCACCCCCTTTAATCATTATTGTTTCACAAATAGTCACAATC-3′) were annealed to form the probe RAP-RRE; LGH4272 (5′-GATCCTTCCAAAAATGGGTGGCTAACCTGTCCAAAATATGGGAAC-3′) and LGH4273 (5′-GATCGTTCCCATATTTTGGACAGGTTAGCCACCCATTTTTGGAAG-3′) were annealed to form probe PAN-RRE; and LGH4274 (5′-GATCCTTCCAAAAATGGGTG**T**CTA**C**CC**GTG**CCAAAATATGGGAAC-3′) and LGH4275 (5′-GATCGTTCCCATATTTTGG**CAC**GG**G**TAG**A**CACCCATTTTTGGAAG-3′) were annealed to form probe PAN-PM1.

Indirect IFA. The IFA was performed at 40 h after transfection of BCBL-1 cells. Procedures for IFA and fluorescence microscopy were described previously (50). Secondary donkey- or goat-derived fluorescein isothiocyanate- or rhodamine-conjugated anti-rabbit or anti-mouse immunoglobulin G (Jackson Pharmaceuticals, West Grove, Pa.) was used to detect the primary antibodies, which included rabbit antipeptide antiserum against KSHV RAP (50) and mouse

anti-Flag monoclonal antibody (MAb) (Sigma). Mounting solution with 4′,6′-diamidino-2-phenylindole (DAPI) (Vector Shield) was used to visualize cellular DNA.

Recombinant protein expression and in vitro GST affinity binding assay. GST fusion protein expression was induced in *Escherichia coli* (strain BL21) with 1 mM isopropyl-β-D-thiogalactopyranoside (IPTG) for 4 h at 30°C. Bacterial pellets were resuspended in ice-cold phosphate-buffered saline (PBS) (150 mM NaCl, 16 mM Na_2HPO_4, 4 mM NaH_2PO_4 [pH 7.3]) and sonicated for 30 s. After centrifugation, clarified lysates were either analyzed by SDS-PAGE or immobilized on glutathione-Sepharose 4B beads (Amersham Pharmacia). Purified GST proteins can be stored at −80°C in 20% glycerol–PBS. Input [^{35}S]methionine-labeled proteins were synthesized in vitro by using the TNT quick coupled transcription-translation system as described above. Recombinant GST fusion proteins immobilized on beads were pretreated with 0.2 U of DNase I and 0.2 μg of RNase A per μl for 30 min at 20°C in pretreating buffer (50 mM Tris-HCl [pH 8.0], 5 mM $MgCl_2$, 2.5 mM $CaCl_2$, 100 mM NaCl, 5% glycerol, 1 mM dithiothreitol). The beads were washed twice with binding buffer (20 mM Tris-Cl [pH 7.5], 100 mM NaCl, 1 mM EDTA, 0.5% NP-40, 1 mM dithiothreitol) and blocked in the same buffer containing 10 mg of bovine serum albumin (BSA)/ml for 30 min at 4°C. After blocking, the bead-immobilized GST fusion proteins were resuspended in binding buffer containing 1 mg of BSA/ml, and labeled proteins were added and incubated for 1 h at 4°C. The beads were washed five times in binding buffer at 10-min intervals. The beads were resuspended in 15 μl of 2× SDS gel loading buffer and boiled for 5 min before loading on SDS-polyacrylamide gels. After electrophoresis, the gels were fixed in 50% methanol–40% H_2O–10% acetic acid for 30 min and dried for X-ray autoradiography.

For in vitro coimmunoprecipitation, 5 to 10 μl of [^{35}S]methionine-labeled in vitro-translated proteins was incubated with 2 μg of mouse anti-c-Myc antibody (Sigma) in 100 μl of immunoprecipitation buffer (50 mM Tris-Cl [pH 7.9], 50 mM NaCl, 0.1 mM EDTA, 1% glycerol, 0.2% NP-40, 1 mM dithiothreitol, 0.5 mM PMSF) for 1 h at 4°C. Then, 50 μl of a 50% slurry of protein A-protein G (50:50) and Sepharose beads (Amersham Pharmacia) was added to the mixture and incubated for 1 h at 4°C. The beads were washed three times with cold immunoprecipitation buffer at 15-min intervals, resuspended and boiled in 2× SDS gel loading buffer, and analyzed by SDS-PAGE followed by autoradiography.

In vivo coimmunoprecipitation and Western immunoblot assay. Nuclear extracts of BCBL-1 cells were prepared for coimmunoprecipitation as described previously (50a). Approximately10^8 cells were harvested 30 h after TPA induction, washed once with PBS, and gently resuspended in 10 ml of cold hypotonic buffer A (10 mM HEPES [pH 7.9], 10 mM KCl, 0.1 mM EDTA, 0.1 mM EGTA, 1 mM dithiothreitol, 0.5 mM PMSF). The mixture was allowed to swell on ice for 30 min, and NP-40 was added to a final concentration of 0.62%. The mixture was vortexed vigorously for 10 s, and the nuclear pellets were collected after centrifugation for 3 min at 3,500 rpm and 4°C. The nuclear pellets were resuspended in 3 ml of cold immunoprecipitation buffer and sonicated for 2 s at the minimal setting. The samples were centrifuged at 13,000 rpm for 1 min at 4°C, and the supernatants were collected as nuclear extracts.

For coimmunoprecipitation, 400 μl of prepared nuclear extracts was pretreated with 0.2 U of DNase I and 0.2 μg of RNase A per μl and precleared with 5 μl of goat or rabbit preimmune serum and 100 μl of a 50% slurry of protein A-protein G (20:80) and Sepharose beads for 1 h. After preclearing, 3 μg of anti-C/EBPα goat polyclonal antibody (PAb), anti-RAP or anti-RTA rabbit PAb, or goat or rabbit preimmune serum was added to the precleared nuclear extracts and incubated for 2 h at 4°C. Then, 100 μl of a 50% slurry of protein A-protein G (20:80) and Sepharose beads blocked with 5% BSA in PBS was added to the nuclear extracts and incubated for 1 h at 4°C. The beads were washed three times with cold immunoprecipitation buffer at 15-min intervals, resuspended in 2× SDS gel loading buffer, and boiled for 5 min before loading on SDS-polyacrylamide gels. Western blot analysis was performed as described previously (50). Any recovered RTA was then detected by immunoblotting with rabbit antiserum raised against a synthetic peptide representing the KSHV RTA segment between amino acids 527 and 539 (NH_2-527-KKRKALTVPEADT-539-COOH).

ChIP assay. The procedures for the chromatin immunoprecipitation (ChIP) assay were modified from the original protocol (1). After treatment of 20 ml of KSHV-positive JSC-1 cells (5×10^6 cells) with TPA (20 ng/ml) for 40 h, 2 ml of formaldehyde solution (11% formaldehyde, 0.1 M NaCl, 1 mM EDTA, 50 mM HEPES [pH 8.0]) was added to the culture and incubated at 37°C for 30 min. The cross-linking reaction was stopped by the addition of 4 ml of 1 M glycine (final concentration, 0.125 M) to the cell culture mixture. After centrifugation, the cell pellets were washed once with 5 ml of cold wash buffer [5 mM piperazine-*N*,*N*′-bis(2-ethanesulfonic acid) (PIPES) (pH 8.0), 85 mM KCl, 0.5% NP-40, 1 mM PMSF, 1 μg of aprotinin/ml, 1 μg of pepstatin/ml]. The cell pellets were resuspended in 500 μl of sonication buffer (1% SDS, 10 mM EDTA, 50 mM Tris-Cl [pH 8.0], 1 mM PMSF) at 20°C in a 1.5-ml microtube and sonicated for 30 s at the minimal setting to shear genomic DNA to ~400-bp fragments. The sonicated mixture (500 μl) was diluted with 5 ml of a cold buffer containing 0.01% SDS, 1.1% Triton X-100, 1.2 mM EDTA, 16.7 mM Tris-Cl (pH 8.0), 167 mM NaCl, and 1 mM PMSF and was precleared with 120 μl of 50% protein A-protein G–Sepharose beads for 8 h at 4°C. After centrifugation to pellet the Sepharose beads, the supernatants were divided into 500-μl aliquots and stored at −70°C for later use.

For each immunoprecipitation assay, 1 μl of KSHV RTA antiserum, 1 μl of KSHV RAP antiserum, 1 μg of anti-C/EBPα PAb (Santa Cruz), 1 μg of anti-EBV ZTA MAb (Argene, N. Masepequa, N.Y.), or 1 μl of PBS (negative control) was added to each 500-μl supernatant aliquot and incubated at 4°C for 2 h with constant mixing. Then, 30 μl of 50% protein A-protein G–Sepharose beads was added to each mixture and incubated at 4°C for 4 h with constant mixing. For protein preclearing experiments, the same mixture was incubated with antibody and protein A-protein G–Sepharose beads at 4°C overnight, and supernatants were collected for a second round of immunoprecipitation. After centrifugation and the removal of supernatants, the Sepharose beads were washed once with 1 ml of dilution buffer at 20°C for 3 min. The beads were washed twice with 1 ml of dilution buffer at 4°C for 20 min each, washed three times with 1 ml of dilution buffer at 20°C for 3 min each, and resuspended in 100 μl of Tris-EDTA (pH 8.0) (TE). RNase A (50 μg/ml) was added, followed by incubation at 37°C for 30 min; then, 5 μl of 10% SDS and 50 μl of proteinase K (500 μg/ml) were added, followed by incubation for 4 h at 37°C with occasional mixing. The same mixture was incubated at 65°C overnight to reverse the cross-linked DNA-protein complex. After centrifugation, supernatants were transferred to new microtubes, diluted with 100 μl of fresh TE, and extracted with equal volumes of phenol and then chloroform. DNA was precipitated with ethanol, and the rinsed and vacuum-dried pellets were resuspended in 100 μl of TE.

For PCR detection, 2 μl of each DNA-TE solution was used as a template. For detection of the immunoprecipitated KSHV RAP promoter region, two primers, LGH4361 (5′-GATCCGCGGATCCAGTTTGGTGCAAAGTGGAGT-3′) and LGH4362 (5′-GATCCGCGGATCCTGGCAGGGTTACACGTTTAC-3′), specific for a 164-bp region in the KSHV RAP promoter that encompasses the C/EBP binding sites and the RRE, were used for PCR amplification. For detection of the KSHV RTA coding region, two primers, LGH4930 (5′-TTCGCCT GTTAGACGAAGC-3′) and LGH4929 (5′-GATTCGCAAGCTTCAGTCTCG GAAGTAATTACG-3′), specific for the RTA coding region from amino acids 591 to 691, were used as a negative control to detect a nonpromoter region. The PCR products were analyzed on a 2.5% agarose gel. Quantification of the PCR products was conducted with a MultiImage light cabinet (Alpha-Innotech Corp.) and the accompanying FluorChem (version 1.02) software.

RESULTS

C/EBPα and KSHV RTA cooperatively activate the RAP promoter. To examine factors that induce RAP expression during the KSHV lytic cycle, a target LUC reporter gene driven by the KSHV RAP promoter region (between positions −190 and +10) was cotransfected into a variety of cell lines along with different combinations of effector mammalian cDNA expression plasmids. Initially, a KSHV RTA expression plasmid was used as a positive control. The addition of just 0.25 μg resulted in 12-fold activation of the RAP promoter-driven reporter gene in Vero cells and 39-fold activation in HeLa cells. This effect was dose responsive, with activation of the RAP promoter reaching 42-fold in Vero cells and 105-fold in HeLa cells when 1 μg of the RTA expression plasmid was used (Fig. 1A and B). Similarly, electroporation of RTA into DG75 lymphocytes resulted in 40-fold activation at the lowest dose (2.5 μg) and 120-fold activation at the highest dose (10 μg) (Fig. 1C).

We then examined whether C/EBPα has any role in activating the RAP promoter, and we found that transfection of C/EBPα alone at the lowest dose resulted in 19-fold activation of the RAP promoter-driven reporter gene in Vero cells, 27-

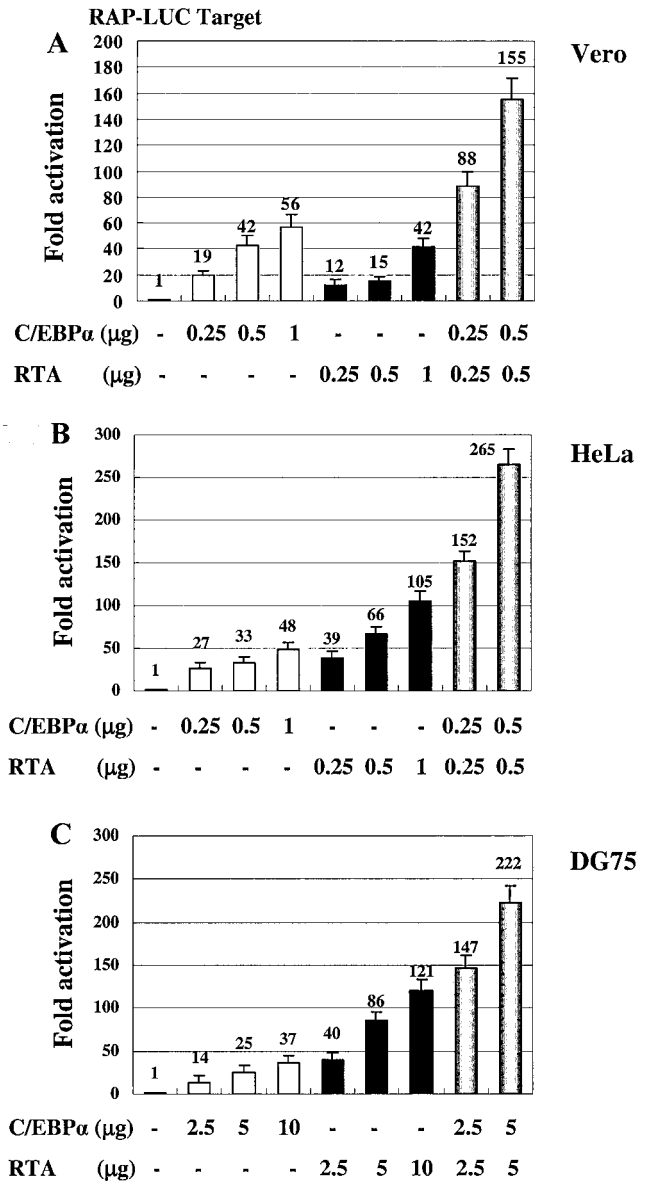

FIG. 1. C/EBPα enhances the transcriptional activation of the KSHV RAP promoter by RTA. Histograms plot the results of dose-response LUC assays in which the target RAP(−190/+10)-LUC reporter gene was transiently expressed either alone or in the presence of mammalian expression plasmids encoding full-length C/EBPα (open bars), RTA (solid bars), or both (gray bars). (A) Cotransfection in Vero cells with Lipofectamine. (B) Cotransfection in HeLa cells with Lipofectamine. (C) Electroporation into KSHV-negative DG75 B lymphocytes.

fold activation in HeLa cells, and 14-fold activation in DG75 cells. Again, the level of RAP promoter activation was proportional to the amount of C/EBPα DNA used, with 56-fold activation in Vero cells, 48-fold activation in HeLa cells, and 37-fold activation in DG75 cells being observed at the highest doses used (Fig. 1).

When both C/EBPα and RTA were added together to the cotransfection mixture, we observed an overall 4- to 5-fold increase; levels reached 88-, 152-, or 147-fold activation of the RAP promoter in Vero, HeLa, or DG75 cells, respectively, with 0.25 μg of each (2.5 μg in DG75 cells) and 155-, 265-, and 222-fold activation in the same cell types, respectively, with 0.5 μg of each (5 μg in DG75 cells) (Fig. 1). These data indicated that in addition to KSHV RTA, C/EBPα is another potent up-regulator of the KSHV RAP promoter in cotransfection assays and that the two transcriptional activators together produce 2.5- to 3-fold additional cooperativity over simple additive effects.

The RAP promoter contains a C/EBPα binding site that binds C/EBPα strongly in vitro. Because C/EBPα itself activated the KSHV RAP promoter, we decided to investigate whether any C/EBP DNA binding sites exist in the RAP promoter. Careful inspection revealed two putative oppositely oriented core C/EBPα binding sites in the RAP promoter region between positions −89 and −67. These two sites, designated C/EBP-I and C/EBP-II (Fig. 2A), contain the ACAAT consensus sequence that is homologous to a half-site of several known palindromic C/EBPα binding sites, although in this case they are located 13 bp apart (perhaps equivalent to one full turn of the helix) and may constitute a double ACAAT palindromic C/EBP binding site. To test the functionality of these putative C/EBP binding sites in binding to C/EBPα in vitro, we performed an EMSA with in vitro-translated C/EBPα and a 33-bp ^{32}P-radiolabeled oligonucleotide probe (RAP-PWT) that encompasses both motifs (C/EBP-I and C/EBP-II). Indeed, with added C/EBPα, we found a single strongly gel-shifted band, suggesting that C/EBPα can bind to this probe very efficiently (Fig. 2B, lane 2). The specificity of this binding by C/EBPα was further confirmed by a supershift of the DNA-protein complex with anti-C/EBPα PAb (Fig. 2B, lane 3).

To evaluate the contributions of the two potential half-sites individually, we generated three mutant probes by selectively destroying one or both of the ACAAT sites. When RAP-PM1 (containing a mutation of C/EBP-I), RAP-PM2 (containing a mutation of C/EBP-II), and RAP-PM1 + 2 (containing both half-site mutations) were used for EMSAs (Fig. 2A), we found that only RAP-PM1 still bound C/EBPα strongly (Fig. 2B, lanes 5 and 6), whereas RAP-PM2 lost 90% of C/EBPα binding ability compared to RAP-PWT (Fig. 2B, lanes 8 and 9). RAP-PM1 + 2, which lacks both the C/EBP-I and the C/EBP-II motifs, failed to bind to C/EBPα at all (Fig. 2B, lanes 11 and 12). Therefore, the concept of a novel palindromic site seems unlikely. Instead, the C/EBP-II motif is the most critical site for binding to C/EBPα, whereas the C/EBP-I motif is bound only weakly and may be nonessential but may still contribute toward overall C/EBPα activity at high protein concentrations.

To test the functionality of these C/EBP binding sites in terms of the ability of C/EBPα to activate the RAP promoter, we generated three mutant RAP(−190/+10)-LUC reporter genes that contained the same sequence mutations as those found in the RAP-PM1, RAP-PM2, and PAP-PM1 + 2 oligonucleotides (Fig. 2A). LUC assays were performed with HeLa cells to evaluate the responsiveness of these individual target mutant RAP promoter genes to transfected effector plasmids expressing C/EBPα, RTA, or both. In comparison to the wild-type RAP(PWT)-LUC reporter, RAP(PM1)-LUC, which contains a mutated C/EBP-I motif, showed only a slight decrease in C/EBPα activation, from 33- to 23-fold, whereas RTA acti-

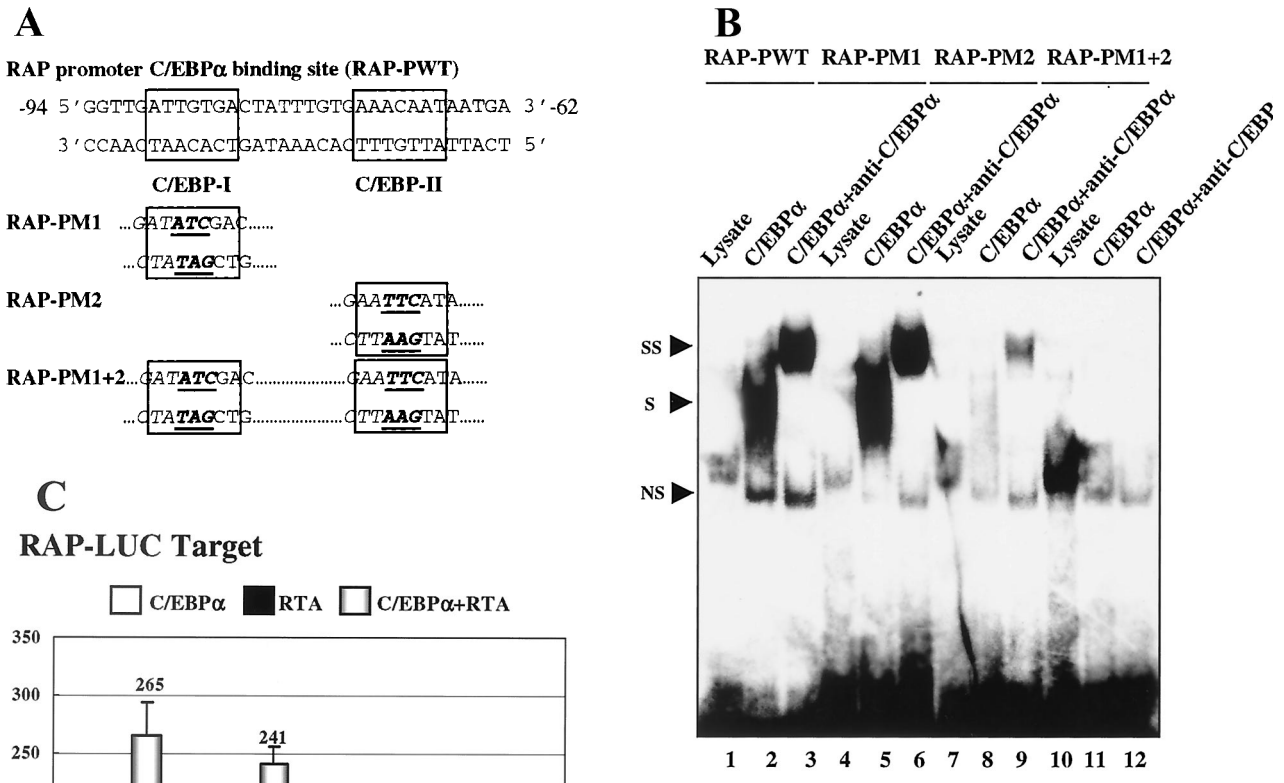

FIG. 2. C/EBPα binds to a proximal region on the KSHV RAP promoter and transactivates RAP expression. (A) Diagram showing the locations of the two putative C/EBP binding sites, C/EBP-I and C/EBP-II, as well as site-specific mutations (underlined, bold) within these two motifs. (B) EMSA experiment showing that in vitro-translated C/EBPα bound strongly to a synthetic ^{32}P-labeled oligonucleotide probe containing the C/EBP-II motif but only weakly to the more distal C/EBP-I motif and that double mutation of both motifs abolished C/EBPα binding. SS, supershifts; S, shifts; NS, nonspecific shifts. (C) Transient LUC reporter gene assay showing that the C/EBP-II motif was essential for C/EBPα-mediated transactivation and synergy. Effector plasmids encoding C/EBPα, RTA, or both were cotransfected into HeLa cells with target reporter plasmids containing either the intact RAP(−190/+10)-LUC reporter gene or its site-specific mutant derivatives RAP-(PM1)-LUC, RAP-(PM2)-LUC, and RAP-(PM1 + 2)-LUC. Numbers on the *y* axis show fold activation.

vation increased from 66- to 96-fold; the cooperativity between RTA and C/EBPα was not seriously affected (Fig. 2C). However, activation by C/EBPα alone was reduced from 33- to 11-fold when RAP(PM2)-LUC, lacking the C/EBP-II motif, was used (Fig. 2C). Furthermore, the cooperativity between RTA and C/EBPα was completely abolished for RAP(PM2)-LUC, with activation dropping from 265-fold in the wild type to 22-fold. Interestingly, activation by RTA alone was also impaired with RAP(PM2)-LUC, dropping from 66-fold for the wild type to 23-fold (Fig. 2C). Finally, the double mutant RAP(PM1 + 2)-LUC also showed reduced C/EBPα and RTA activation, and the C/EBPα-RTA synergy was completely abolished (Fig. 2C). These results showed that the C/EBP-II binding site not only is important for both C/EBPα and RTA to activate transcription of the RAP gene but also is essential for the cooperativity between RTA and C/EBPα. The considerable residual C/EBPα and RTA activation of RAP(PM2)-LUC and RAP-(PM1 + 2)-LUC suggests that there may also be weaker but noncooperative target sites for both proteins elsewhere in the RAP promoter. Indeed, we found that deletion of additional upstream sequences, from −190 to −140, in the wild-type RAP promoter-LUC reporter gene reduced RTA responsiveness nearly twofold (data not shown).

RTA and the RRE. KSHV RTA was previously reported to target a 16-bp region on the KSHV RAP promoter known as the RAP RRE (25, 45), but unexpectedly this site proved to overlap the critical C/EBP-II motif that we identified above. The defined RAP RRE contains the sequence GTGAAACA ATAATGATT, of which the underlined portion (AAACAAT) represents the core C/EBP-II motif (Fig. 3A). When the C/EBP-II motif was mutated in the RAP promoter reporter gene (RAP-PM2), not only did the promoter show reduced responses to both C/EBPα and RTA transactivation, but also the synergy exhibited between C/EBPα and RTA was completed abolished (Fig. 2B). Therefore, our data suggested that direct RTA activation of the RAP promoter is at least partially

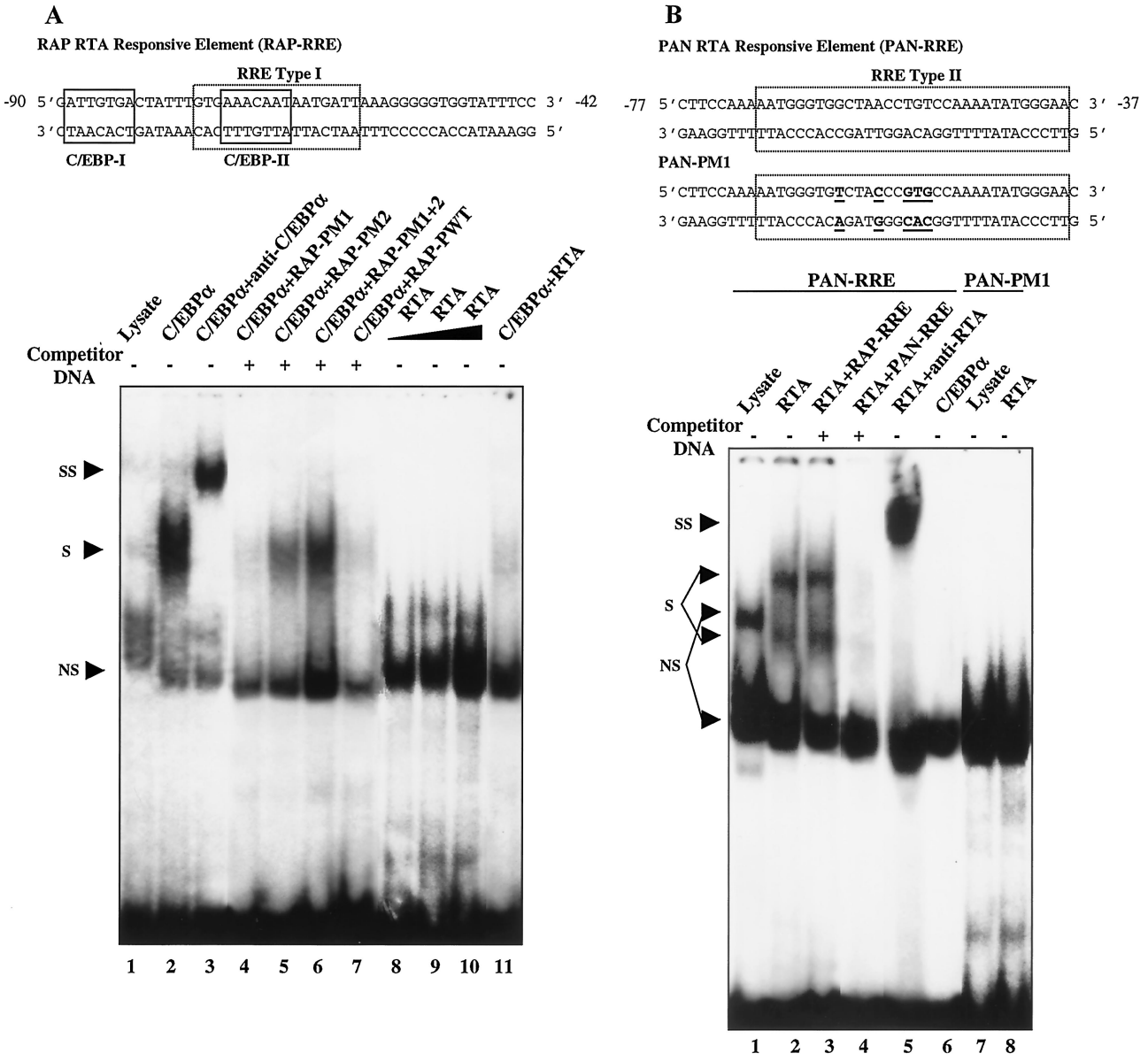

FIG. 3. The C/EBP binding site in the RAP promoter overlaps the KSHV RAP promoter type I RRE sequence, which has only weak affinity for in vitro-translated RTA, compared to the high-affinity type II RRE sequence from the KSHV PAN promoter. (A) (Upper panel) Sequence of the 49-bp oligonucleotide probe (RAP-PWT) containing both of the C/EBP binding sites and overlapping the RTA type I RRE sequence from the RAP promoter (RAP-RRE). (Lower panel) EMSA with ^{32}P-labeled probe RAP-RRE and in vitro-translated proteins. Lane 1, control reticulocyte lysate (2 μl) alone did not bind to probe RAP-RRE. Lanes 2 and 3, binding of in vitro-translated C/EBPα (2 μl) to probe RAP-RRE and supershifting of the C/EBPα gel shift with anti-C/EBPα PAb (0.5 μl). Lanes 4 to 7, C/EBPα (2 μl) binding could be competed away with unlabeled oligonucleotides (100-fold excess) containing the wild-type C/EBP-II motif (RAP-PM1 and RAP-PWT) but not with RAP-PM2 or RAP-(PM1 + 2), each of which contains the mutant C/EBP-II motif. Lanes 8 to 10, dose-response assay showing that in vitro-translated RTA (2, 4, and 6 μl, respectively) failed to bind to probe RAP-RRE even with increasing amounts of RTA. Lane 11, loss of the C/EBPα (2 μl) complex bound to the RAP RRE after the addition of in vitro-translated RTA (1 μl) (compare with lane 2), suggesting a physical interaction between the two proteins. SS, supershifts; S, shifts; NS, nonspecific bands. (B) (Upper panel) Sequences of the 41-bp oligonucleotide probe (PAN-RRE) containing the RTA type II RRE from the PAN promoter and of a mutated version of the RRE (PAN-PM1). Underlining and bold type indicate mutations. (Lower panel) EMSA with ^{32}P-labeled PAN RRE probes and in vitro-translated proteins. Lane 1, control reticulocyte lysate (2 μl) did not harbor any probe PAN-RRE binding activity. Lane 2, in vitro-translated RTA (4 μl) bound to probe PAN-RRE. Lane 3, unlabeled oligonucleotide RAP-PWT (100-fold excess) did not compete away RTA binding to labeled probe PAN-RRE. Lane 4, unlabeled oligonucleotide PAN-RRE (100-fold excess) completely competed away RTA binding to labeled probe PAN-RRE. Lane 5, supershift of the DNA-bound RTA band with anti-RTA PAb (1 μl), confirming the identity of the RTA shifts. Lane 6, negative control showing that C/EBPα (2 μl) did not bind to probe PAN-RRE. Lanes 7 and 8, neither the negative control reticulocyte lysate (2 μl) nor RTA (4 μl) bound to mutant probe PAN-PM1.

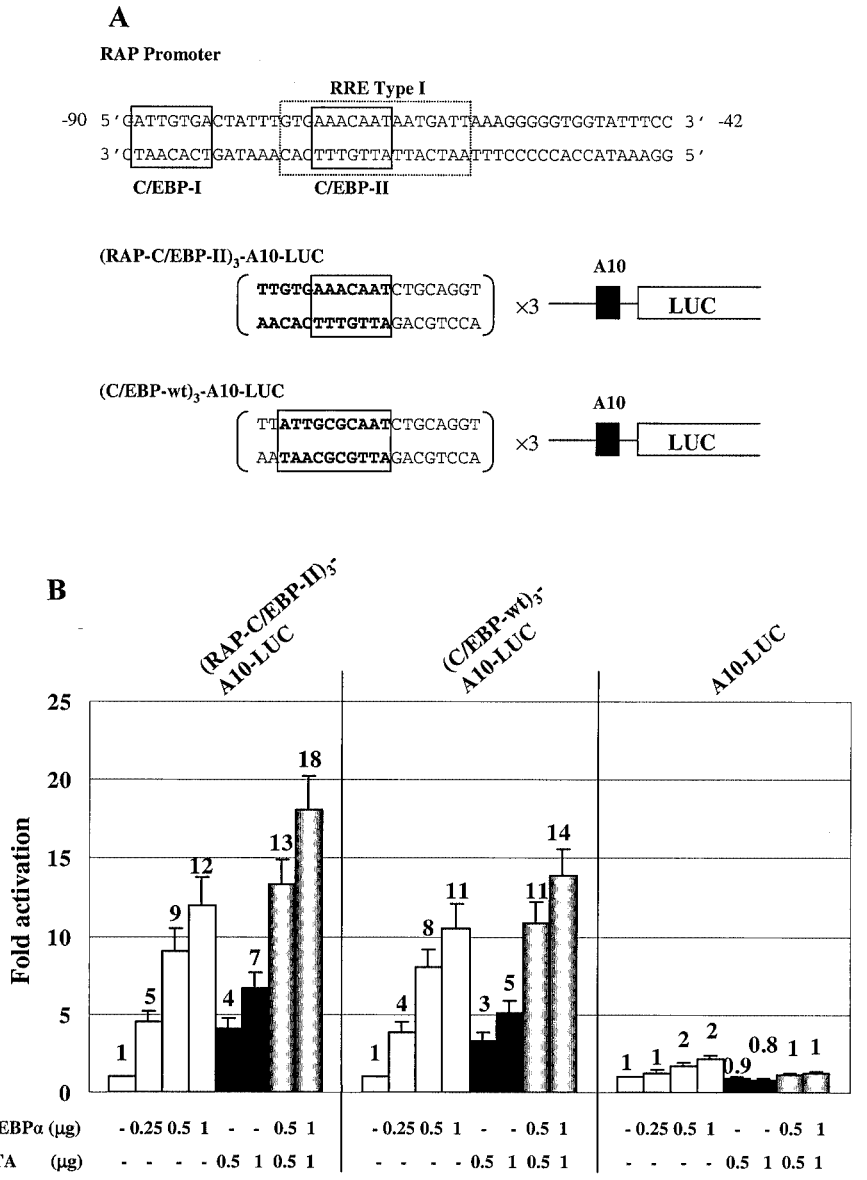

FIG. 4. Transfer of RTA responsiveness by minimal C/EBP binding sites inserted into a heterologous reporter gene background. (A) Schematic showing the inserted 20-bp C/EBP motif oligonucleotides and sequences (bold type) in the target (RAP-C/EBP-II)$_3$-A10-LUC and (C/EBP-wt)$_3$-A10-LUC reporter genes, compared to the wild-type type I RRE motif in the RAP promoter-LUC reporter gene. (B) Histograms plotting the results of dose-response LUC assays in which the target (RAP-C/EBP-II)$_3$-A10-LUC, (C/EBP-wt)$_3$-A10-LUC, and parent A10-LUC reporter genes were transiently expressed in HeLa cells either alone or in the presence of mammalian expression plasmids encoding full-length C/EBPα, RTA, or both.

dependent upon the integrity of the AAACAAT C/EBPα binding sequence and raised questions about a possible physical interaction between C/EBPα and RTA. However, because Lukac et al. have also reported that RTA transactivates the RAP promoter through direct binding of RTA to the RRE (25), we decided to further address these observations by exploring the physical interactions among RTA, C/EBPα, and both type I and type II RRE DNA sequences.

To investigate binding to RAP RRE DNA by both C/EBPα and RTA, a 49-bp oligonucleotide probe encompassing the entire RRE but also containing both potential C/EBP binding sites was tested in EMSA experiments. We found that in vitro-translated C/EBPα was able to bind to probe RAP-RRE very strongly, as expected (Fig. 3A, lanes 2 and 3). To further confirm this phenomenon, unlabeled competitor oligonucleotides (RAP-PWT, RAP-PM1, RAP-PM2, and RAP-PM1 + 2) were added to binding reaction mixtures containing C/EBPα and radiolabeled probe RAP-RRE at a 200-fold excess (Fig. 3A, lanes 6 to 9). Consistent with our previous EMSA results obtained with those mutant oligonucleotides as direct radiolabeled probes, we found that the RAP-PWT and RAP-PM1 oligonucleotides competed efficiently for C/EBPα interactions

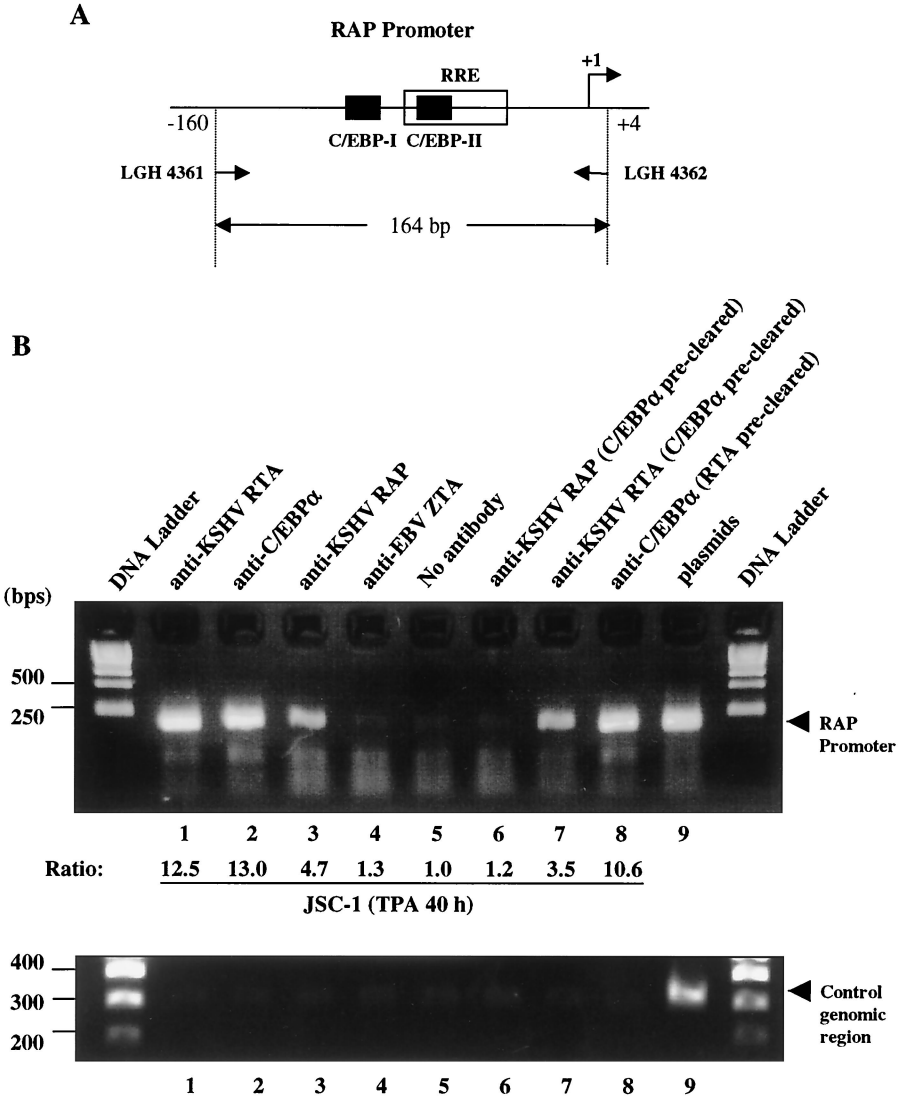

FIG. 5. ChIP assay with JSC-1 cell extracts after 40 h of TPA treatment showing that C/EBPα, RTA, and RAP all associate with the RAP promoter and that C/EBPα is required for RTA and RAP to associate efficiently. (A) Schematic of the 164-bp region of the RAP promoter encompassing both of the C/EBP binding sites and the RRE that was targeted for detection via PCR amplification with two specific primers, LGH4361 and LGH4362. (B) (Upper panel) Lanes 1 to 5, ChIP assay results showing that RAP promoter DNA could be recovered from immunoprecipitates containing either RTA, C/EBPα, or RAP but not from immunoprecipitates with ZTA or a negative control antibody. Lanes 6 and 7, removal of C/EBPα from lysates (preclearing) abolished the association of RAP with the RAP promoter and weakened the association of RTA. Lane 8, association of C/EBPα with RAP promoter DNA was not affected by the removal of RTA. Lane 9, PCR amplification products obtained from the RAP promoter expression plasmid (pFYW41) with the same primers, indicating the expected correct sizes of the PCR products. (Lower panel) Negative control. ChIP assay results showing that nonpromoter DNA fragments were not coprecipitated nonspecifically with these antibodies. Lanes 1 to 9, primers (LGH4929 and LGH4930) specific for the detection of RTA coding region DNA (300 bp) failed to detect any positive signals above the basal level, except from the cDNA plasmid control (lane 9).

against labeled probe RAP-RRE, whereas the RAP-PM2 oligonucleotide showed much weaker competition. The RAP-PM1 + 2 oligonucleotide did not interfere at all with C/EBPα binding to probe RAP-RRE.

Surprisingly, we were unable to observe any interaction between in vitro-translated wild-type RTA and the RAP RRE sequence in our EMSA system (Fig. 3A, lanes 8 to 10). Conceivably, this form of RTA binds to probe RAP-RRE very weakly, and the interaction was not obvious with the low concentrations of RTA obtained by in vitro translation. Therefore, to confirm the functional viability of our in vitro-translated RTA in binding to other target DNA sequences with an affinity for RTA, we tested a different RTA consensus sequence (type II RRE), which was found in the KSHV PAN promoter and which was reported to bind to RTA very strongly (36). A 41-bp oligonucleotide (PAN-RRE) that contained the 32-bp RRE region from the KSHV PAN promoter was used for an EMSA under the same binding conditions. In this experiment, the in vitro-translated wild-type RTA sample bound to probe PAN-RRE and formed two shifted bands (upper band, RTA shift;

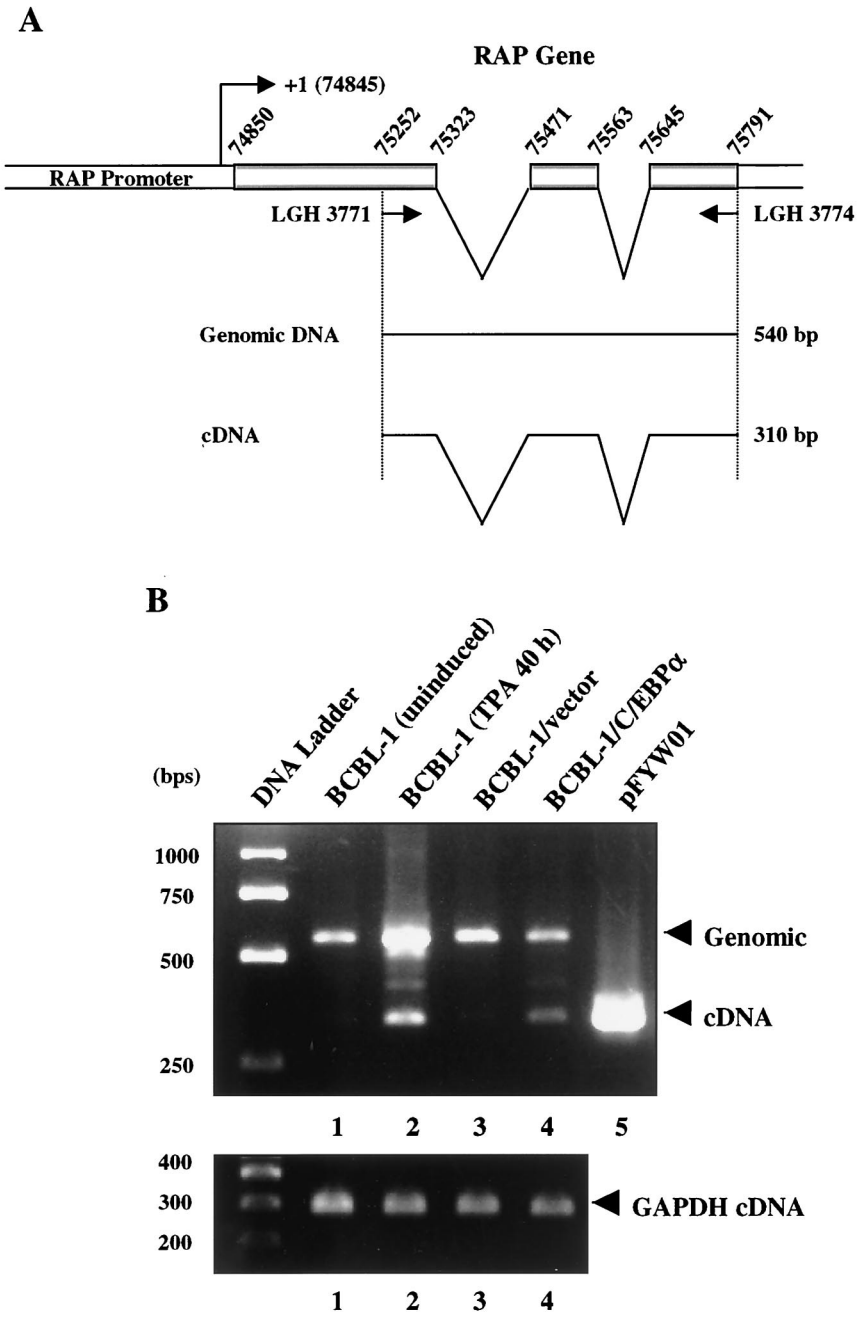

FIG. 6. RT-PCR showing that an exogenously introduced C/EBPα expression vector can trigger RAP transcription in BCBL-1 cells latently infected with KSHV. (A) Schematic showing the splicing pattern for the full-length KSHV RAP mRNA. (B) (Upper panel) RT-PCR performed with mRNA harvested from C/EBPα-transfected BCBL-1 cells and with primers specific for the RAP gene. Lane 1, lack of detectable RAP cDNA in untreated BCBL-1 cells. Lane 2, increased RAP cDNA level in TPA-treated BCBL-1 cells undergoing lytic-cycle induction. Lane 3, lack of detectable RAP cDNA in BCBL-1 cells transfected with empty vector DNA. Lane 4, induction of RAP cDNA in C/EBPα-transfected BCBL-1 cells. Lane 5, positive size marker control showing the PCR products from the RAP cDNA expression plasmid (pFYW01). (Lower panel) Loading and amplification control experiment showing that equal concentrations of template mRNA were used, as illustrated by the uniform levels of glyceraldehyde-3-phosphate dehydrogenase (GAPDH) mRNA RT-PCR products.

lower band, degradation products of RTA shift) that could in turn be supershifted by RTA antiserum (Fig. 3B, lanes 2 and 5). The same RTA sample failed to bind to mutant probe PAN-PM1 (Fig. 3B, lane 8).

LUC reporter gene assays with a cotransfected target PAN promoter (positions −261 to +14) as a control showed that the PAN promoter can be strongly activated by RTA, as expected (see (Fig. 12C). However, despite the ability of C/EBPα to bind to probe RAP-RRE, C/EBPα was unable to recognize the RRE in the PAN promoter and thus was unable to bind to

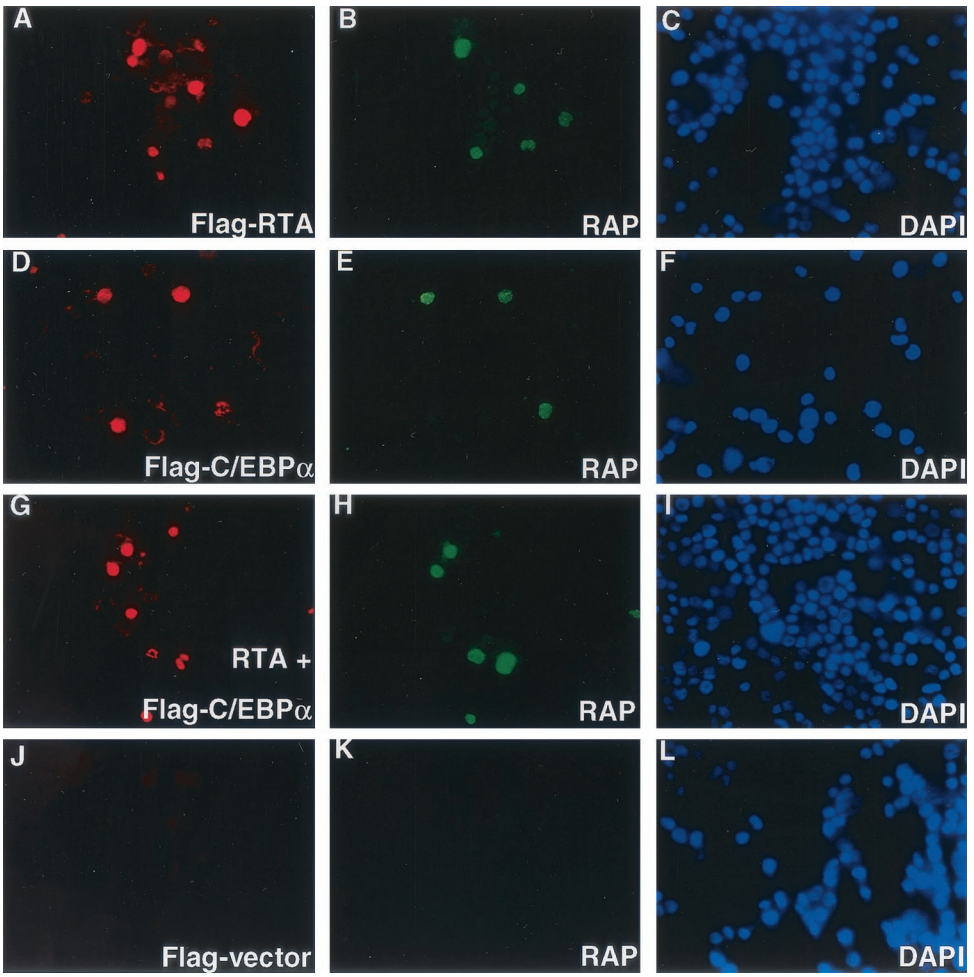

FIG. 7. Both exogenously introduced Flag-RTA and Flag-C/EBPα trigger RAP expression in DNA-transfected BCBL-1 cells. (A to C) Double-label IFA illustrating the expression of Flag-RTA (in SV2-Flag-RTA-transfected cells), as detected with anti-Flag MAb (A, rhodamine, red), and enhanced expression of RAP, as detected in the same cell population with anti-RAP PAb (B, fluorescein isothiocyanate, green). (C) DAPI nuclear staining (blue) showing all cells in the same field. (D to F) Double-label IFA showing the expression of Flag-C/EBPα (in Flag-C/EBPα-transfected cells), as detected with anti-Flag MAb (D, red), and enhanced expression of RAP, as detected in the same cell population with anti-RAP PAb (E, green). (F) DAPI (blue) showing the whole cell population. (G to I) Double-label IFA showing that the cotransfection of both untagged RTA and Flag-tagged C/EBPα, as detected by anti-Flag MAb (G, red), greatly enhanced the induction of endogenous RAP expression (H, green). (I) DAPI (blue) showing the whole cell population. (J to L) Double-label IFA showing the lack of expression from the empty Flag vector (J, red) and the absence of RAP expression (K, green) in the same infected cell population. (L) DAPI (blue) showing the whole cell population. Note that spontaneous background RAP expression occurred in approximately 1% of untreated BCBL-1 cells.

probe PAN-RRE at all in our EMSA experiments (Fig. 3B, lane 6). Furthermore, when probe RAP-RRE, which could not bind to in vitro-translated RTA, and probe PAN-PM1 (Fig. 3B, lane 8), which contained mutations abolishing RTA binding (36), were used as competitors, neither of them was able to interfere with the formation of the RTA complex bound to probe PAN-RRE (Fig. 3B, lane 3, and data not shown). As a positive control, when we used the same amounts of probe PAN-RRE as an unlabeled excess competitor, formation of the bound RTA gel shift complex was abolished (Fig. 3B, lane 4). These results suggested that probe RAP-RRE has only low if any affinity for RTA, whereas probe PAN-RRE has very high affinity, and also proved that our in vitro-translated RTA was capable of binding efficiently to a DNA sequence that contains a type II RRE.

We next examined whether RTA could bind to probe RAP-RRE in EMSA experiments in the presence of C/EBPα. However, when both C/EBPα and RTA were added to a binding mixture containing labeled probe RAP-RRE, C/EBPα binding to probe RAP-RRE was diminished, but no new complexes were observed (Fig. 3A, lane 11). Furthermore, the inhibitory effect was both dose responsive and specific for C/EBPα, in contrast to EBV ZTA, whose DNA binding was not affected by the addition of RAP (data not shown). These results implied either of two possibilities: (i) RTA inhibits C/EBPα binding to the RRE, or (ii) RTA and C/EBPα bind to the RRE cooperatively; however, the RTA-C/EBPα-DNA complex either is too large or is not stably maintained in the in vitro system, leading to the failure to observe a supershift. Assays with target RAP promoter-LUC reporter genes showed that there is cooperativity between RTA and C/EBPα in transactivating the RAP promoter; therefore, unless they both act by removing

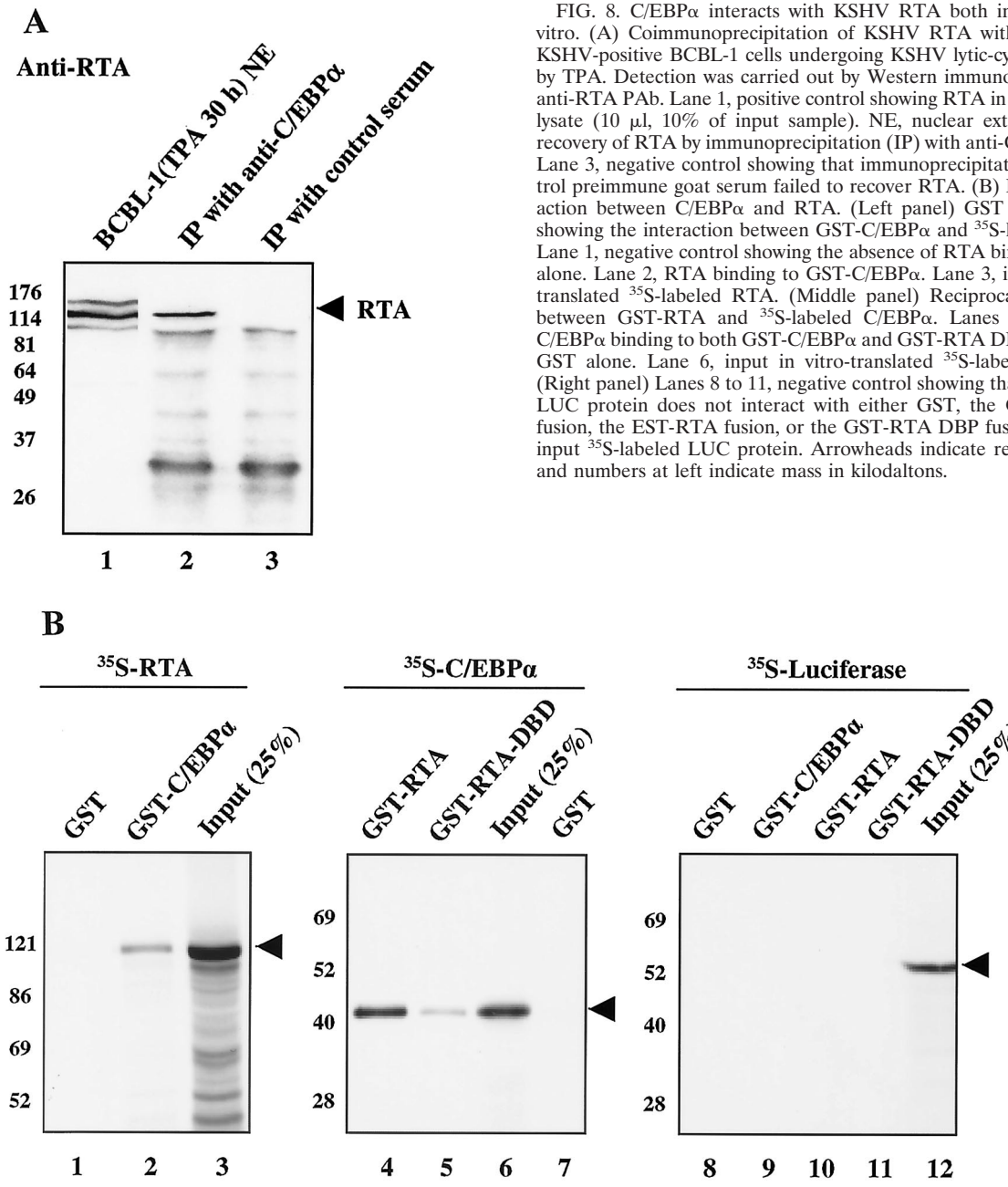

FIG. 8. C/EBPα interacts with KSHV RTA both in vivo and in vitro. (A) Coimmunoprecipitation of KSHV RTA with C/EBPα in KSHV-positive BCBL-1 cells undergoing KSHV lytic-cycle induction by TPA. Detection was carried out by Western immunoblotting with anti-RTA PAb. Lane 1, positive control showing RTA in the input cell lysate (10 μl, 10% of input sample). NE, nuclear extract. Lane 2, recovery of RTA by immunoprecipitation (IP) with anti-C/EBPα PAb. Lane 3, negative control showing that immunoprecipitation with control preimmune goat serum failed to recover RTA. (B) In vitro interaction between C/EBPα and RTA. (Left panel) GST affinity assay showing the interaction between GST-C/EBPα and ^{35}S-labeled RTA. Lane 1, negative control showing the absence of RTA binding to GST alone. Lane 2, RTA binding to GST-C/EBPα. Lane 3, input in vitro-translated ^{35}S-labeled RTA. (Middle panel) Reciprocal interaction between GST-RTA and ^{35}S-labeled C/EBPα. Lanes 4, 5, and 7, C/EBPα binding to both GST-C/EBPα and GST-RTA DBD but not to GST alone. Lane 6, input in vitro-translated ^{35}S-labeled C/EBPα. (Right panel) Lanes 8 to 11, negative control showing that ^{35}S-labeled LUC protein does not interact with either GST, the GST-C/EBPα fusion, the EST-RTA fusion, or the GST-RTA DBP fusion. Lane 12, input ^{35}S-labeled LUC protein. Arrowheads indicate reactive bands, and numbers at left indicate mass in kilodaltons.

inhibitory binding proteins, it seems more likely that a DNA-bound RTA-C/EBPα supercomplex is formed in vivo but cannot be maintained stably during in vitro EMSA experiments. Note that the addition of either RAP or EBV ZTA to C/EBPα in EMSA experiments also led to abolition of the C/EBPα gel-shifted band without the formation of detectable stable supershifted bands (49; Wu et al., unpublished).

Responsiveness of minimal C/EBP binding sites to RTA activation. To evaluate the possibility that just the core C/EBP binding site or another consensus C/EBP binding site in a heterologous background would also confer RTA responsiveness, we constructed two additional target LUC reporter genes in a minimal simian virus 40 promoter background (pA10-LUC). The (RAP-C/EBP-II)$_3$-A10-LUC gene contained three inserted tandem copies of the minimal C/EBP-II motif (AAA CAAT) found in the RAP promoter but without the adjacent segment of the previously defined RRE sequence (AATGA TT) (Fig. 4A), and the (C/EBP-wt)$_3$-A10-LUC gene contained three inserted tandem copies of a consensus palindromic C/EBP binding site (ATTGCGCAAT) (43) (Fig. 4A). The minimal construct pA10-LUC, used as a negative control, showed no significant responsiveness to either C/EBPα or RTA (Fig. 4B). However, C/EBPα activated (RAP-C/EBP-II)$_3$-A10-LUC 12-fold, and RTA activated the same promoter in a dose-responsive manner up to 7-fold, although in the presence of both RTA and C/EBPα the activation level was

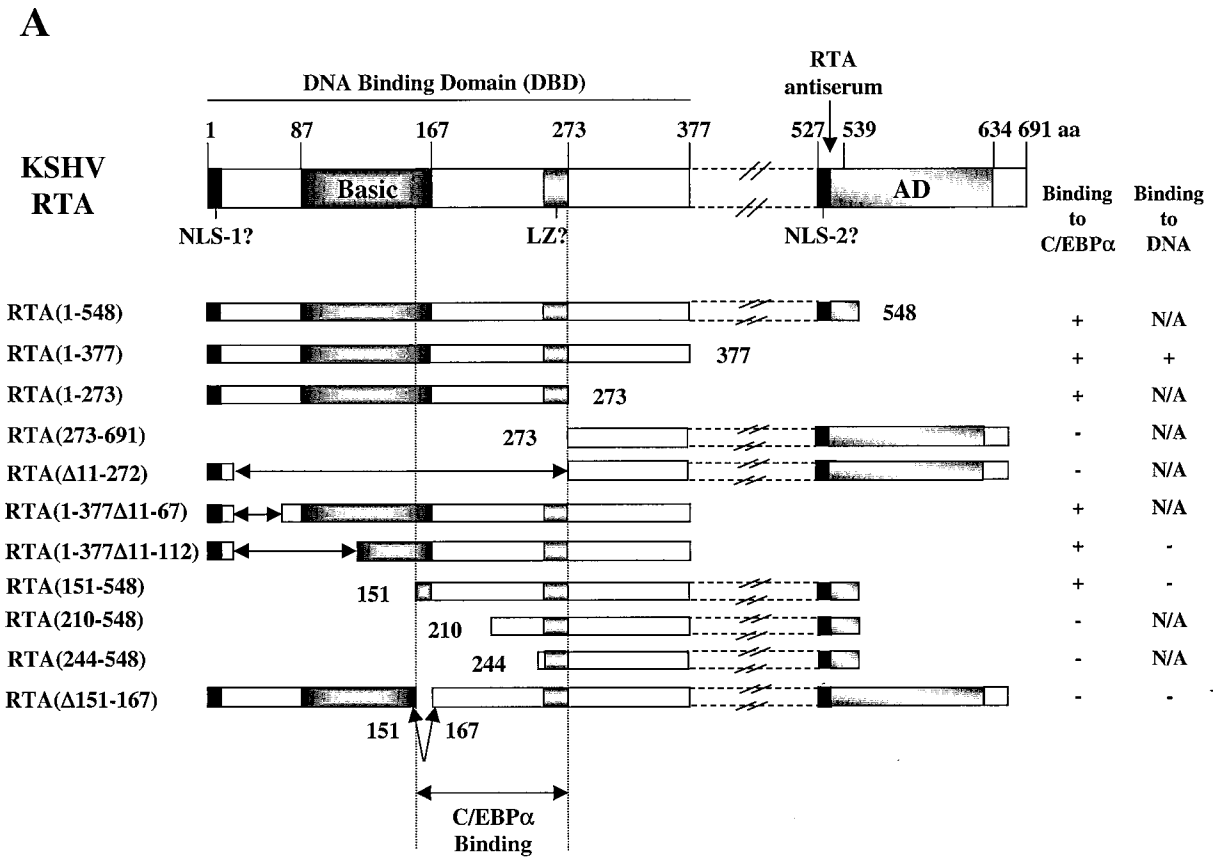

FIG. 9. C/EBPα interacts with a domain of RTA mapping between amino acids 151 and 273. (A) Diagram of wild-type RTA and RTA deletion mutants used. aa, amino acid; NLS, nuclear localization sequence; LZ, leucine zipper domain; AD, activation domain; N/A, not tested. (B) Relative sizes and abundances of the 10 ^{35}S-labeled in vitro-translated (IVT) proteins used as inputs for GST affinity assays. (C) Results of in vitro GST affinity assays showing the relative levels of different RTA deletion mutants recovered after binding to purified GST-C/EBPα fusion beads. Numbers at left indicate mass in kilodaltons.

only an additive 18-fold (Fig. 4B). Similarly, C/EBPα activated (C/EBP-wt)$_3$-A10-LUC 11-fold, and RTA also activated the consensus palindromic C/EBP binding site in a dose-responsive manner up to 5-fold; however, in the presence of both effectors, the response was increased only additively to 14-fold (Fig. 4B). Obviously, in this heterologous context, compared to in the RAP promoter context, both C/EBPα responsiveness and RTA responsiveness declined greatly. However, the basal level of activity of our A10 minimal promoter was considerably higher than that of the wild-type RAP promoter-LUC reporter gene (data not shown). Therefore, RTA appeared to retain some ability to activate all C/EBP binding sites after transfer to a heterologous context in the absence of the additional specific RAP RRE motif, although the level of activation was much lower than that for the intact RRE itself in the wild-type RAP promoter.

RTA and C/EBPα bind to the RAP RRE cooperatively in vivo, as shown by a ChIP assay. To attempt to confirm our model that an RAP RRE-bound RTA-C/EBPα supercomplex forms in vivo, we performed an in vivo ChIP assay with lytically induced JSC-1 PEL cells. First, we immunoprecipitated RTA, C/EBPα, and RAP from the cross-linked DNA-protein cell lysates; after the removal of all proteins, the recovered DNA was ethanol precipitated and amplified by PCR with primers specific for the RAP promoter (LGH4361 and LGH4362). RAP promoter DNA was indeed found to be associated with each of the RTA, C/EBPα, and RAP immunoprecipitates (Fig. 5B, lanes 1 to 3). The negative controls with anti-EBV ZTA antibody or with PBS failed to precipitate any RAP promoter DNA (within basal levels) (Fig. 5B, lanes 4 and 5). To address the question of whether RTA and C/EBPα may bind to RAP RRE DNA cooperatively, we precleared C/EBPα from lysates with anti-C/EBPα PAb overnight and then reimmunoprecipitated RTA with RTA antiserum in a second round. The results showed that RAP promoter DNA could still be recovered from the RTA immunoprecipitate in the second round (Fig. 5B, lane 7), although at a level more than threefold lower (ratio of 3.5 versus 12.5) than that obtained when C/EBPα was present in lysates. A parallel control second immunoprecipitation with C/EBPα confirmed that over 95% of the C/EBPα-bound DNA was removed (data not shown). These results suggested that, although the removal of C/EBPα significantly impaired the ability of RTA to bind to RAP promoter DNA, some RTA was still able to associate with the RAP promoter, although much less efficiently. Furthermore, the removal of RTA by antibody preclearing did not significantly affect the association of C/EBPα with RAP promoter DNA (Fig. 5B, lane 8). These results suggested that, although C/EBPα contributed to the

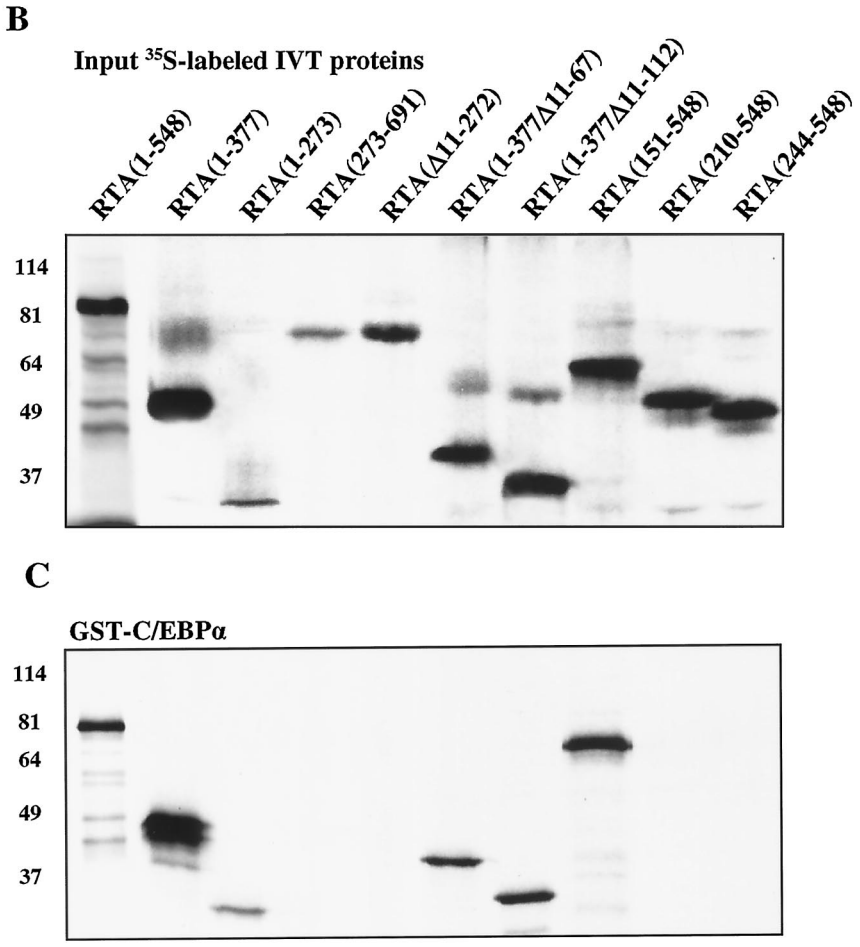

FIG. 9—*Continued*.

binding of RTA to the RAP RRE, RTA did not seem to play a major reciprocal role in mediating the binding of C/EBPα to the RAP RRE. This conclusion is consistent with our earlier EMSA data which showed that, in contrast to RTA alone, in vitro-translated C/EBPα alone bound to probe RAP-RRE very efficiently. Therefore, our ChIP assay data support the model that most of the RTA binding to RAP RRE DNA requires a cooperative interaction with C/EBPα.

Unexpectedly, we also observed an association of RAP with RAP promoter DNA (Fig. 5B, lane 3), although the level was relatively weak compared to those obtained with RTA and C/EBPα (ratio of 4.7 versus 12.5 and 13.5, respectively). Because RAP interacts with C/EBPα, the ChIP assay data suggested that RAP may become associated with DNA indirectly through binding to DNA-bound C/EBPα. To address the question of whether any RAP would still be associated with RAP promoter DNA in the absence of C/EBPα, we precleared C/EBPα from cell lysates with anti-C/EBPα antibody and protein A-protein G–Sepharose and used the supernatants for a second round of immunoprecipitation with anti-RAP PAb. Indeed, after the removal of C/EBPα, we failed to recover any RAP promoter DNA with anti-RAP PAb (similar to the basal level) (Fig. 5B, lane 6). This result suggested that RAP interacts here only with DNA-bound C/EBPα and that, after the removal of C/EBPα in the preclearing step, no additional RAP was associated with RAP promoter DNA.

A negative control PCR assay with a pair of primers that specifically detected only coding region DNA sequences from within the KSHV RTA gene (LGH4929 and LGH4930) failed to yield any positive signals beyond the background level (Fig. 5B, lower panel). This result confirmed that our ChIP assay was specific and recovered only promoter region DNA sequences specifically bound by the immunoprecipitated proteins.

Expression of C/EBPα induces endogenous RAP mRNA and RAP protein in PEL cells. We have shown by LUC reporter gene assays and by EMSA studies that C/EBPα indeed binds to and transcriptionally activates the RAP promoter in vitro. Therefore, we next examined whether exogenously introduced C/EBPα may be capable of triggering the expression of the RAP gene in infected cells. Total cell mRNA was harvested from BCBL-1 cells latently infected with KSHV after transfection with either a mammalian expression plasmid encoding C/EBPα or an empty vector as a negative control. As a positive control, we also harvested mRNA from TPA-treated BCBL-1 cells, where RAP expression is known to be induced. RT-PCR was then performed to detect changes in the levels of RAP cDNA.

Functional RAP mRNA is the product of differential splicing and consists of three different exons (52). A pair of primers spanning positions 75252 to 75271 (LGH3771) and positions 75774 to 75791 (LGH3774) was designed for PCR of the total cDNA to distinguish the 540-bp RAP genomic DNA fragment from the spliced 310-bp RAP cDNA fragment (Fig. 6A). As expected, in nontransfected BCBL-1 cells (negative control), the 540-bp genomic DNA fragment of RAP was readily apparent, but the cDNA form was barely detectable (Fig. 6B, lane 1); however, in TPA-treated BCBL-1 cells (positive control), both the 540-bp genomic DNA fragment and the 310-bp cDNA fragment of RAP were present at high levels as a result of KSHV lytic-cycle induction and viral DNA replication (Fig. 6B, lane 2). In comparison, cells transfected with the C/EBPα expression plasmid showed significantly induced RAP mRNA expression, as exemplified by the increased level of the RAP cDNA fragment (Fig. 6B, lane 4); however, in cells transfected with the empty expression vector, there was no evidence for the induction of RAP mRNA (Fig. 6B, lane 3). RT-PCR products of glyceraldehyde-3-phosphate dehydrogenase mRNA showed that equal amounts of mRNA were used in the RT-PCR (Fig. 6B, lower panel).

To visually confirm that the expression of RAP was induced specifically only in C/EBPα-positive BCBL-1 cells, we performed IFA experiments. Latently infected BCBL-1 cells were transfected with either a Flag-tagged C/EBPα expression plasmid or a Flag-tagged RTA expression plasmid as a positive control, and RAP expression was monitored by double-stain IFA with anti-RAP rabbit antiserum and anti-Flag MAb. In RTA-transfected BCBL-1 cells, 82% of the Flag-RTA-positive cells were also positive for RAP expression (Fig. 7A to C), confirming that RTA strongly induced RAP expression (25, 45). Similarly, in C/EBPα-transfected BCBL-1 cells, 74% of the Flag-C/EBPα-positive cells were also positive for RAP expression (Fig. 7D to F). Therefore, although this percentage was slightly lower than that for Flag-RTA-positive cells, C/EBPα was clearly also a potent transcriptional activator of the RAP gene in the context of the latent viral genome in PEL cells. Furthermore, in BCBL-1 cells doubly transfected with both untagged RTA and Flag-tagged C/EBPα, 98% of the Flag-positive cells became positive for RAP expression (Fig. 7G to I), suggesting that cooperativity between RTA and C/EBPα contributed to even greater levels of activation of the RAP promoter. As a negative control, BCBL-1 cells transfected with the empty Flag vector produced no increase in RAP expression beyond the low level of the spontaneously lytic population (<2%) (Fig. 7J to L).

C/EBPα physically interacts with KSHV RTA. Because of the cooperativity observed between C/EBPα and RTA in transient reporter gene assays, we examined whether the two proteins could physically interact with each other. We initially examined this interaction by performing a coimmunoprecipitation experiment with KSHV-positive BCBL-1 cells. RTA expression in BCBL-1 cells was induced by TPA-treatment. Nuclear extracts of BCBL-1 cells were prepared 30 h after induction, and an immunoprecipitation experiment was performed with anti-C/EBPα goat PAb. Because both C/EBPα and RTA can bind to DNA, we also included DNase I incubation and added ethidium bromide to the immunoprecipitation reaction to destroy double-stranded DNA and prevent nonspecific protein-protein linking via DNA binding. The immunoprecipitate was analyzed by SDS-PAGE and Western blotting, which detected a 120-kDa band of coprecipitating RTA, indicating that endogenous C/EBPα and RTA strongly interacted with each other in BCBL-1 cells (Fig. 8A, lane 2). A negative control experiment performed with preimmune goat serum yielded no RTA signal (Fig. 8A, lane 3). RTA present in the input nuclear extract yielded at least two distinct bands, but the upper one (150 kDa) was not detected in the immunoprecipitate, perhaps indicating the existence of a modified form of RTA that does not bind to C/EBPα (Fig. 8A, lane 1).

The interaction between RTA and C/EBPα was further confirmed by GST affinity assays with bacterially expressed GST-C/EBPα or GST-RTA recombinant fusions. [^{35}S]methionine-labeled in vitro-translated RTA or C/EBPα samples were added to reaction mixtures containing either GST-C/EBPα or GST-RTA immobilized on glutathione beads. After extensive washing of the beads, bound ^{35}S-labeled C/EBPα or RTA was recovered from the beads, suggesting that a strong interaction occurred between C/EBPα and RTA (Fig. 8B, left and middle panels). In contrast, ^{35}S-labeled in vitro-translated LUC protein used as a negative control failed to interact with either GST-C/EBPα or GST-RTA (Fig. 8B, right panel). Furthermore, a GST-RTA DBD fragment that contained only the N-terminal 377 amino acids of RTA still interacted with C/EBPα, but at a somewhat lower affinity (Fig. 8B, middle panel), suggesting that the interaction with C/EBPα was mediated by the RTA DBD only (see below).

RTA associates with C/EBPα through a basic domain mapping between positions 151 and 170 in RTA. To further confirm and map the RTA domain that interacts with C/EBPα, extensive mutagenesis was performed, and a series of RTA deletion mutants were constructed (Fig. 9A). The expression of all of the RTA deletion mutants was confirmed by [^{35}S]methionione-labeled in vitro translation (Fig. 9B). After testing the abilities of these mutants to interact with GST-C/EBPα by GST affinity assays, we identified a region of RTA, between amino acids 151 and 272 and encompassing a basic domain, that is crucial for the binding of RTA to C/EBPα (Fig. 9C). All RTA deletion mutants containing the first 273 amino acids from the N terminus were able to interact with C/EBPα, and several RTA mutants harboring various deletions in front of position 151 were also able to associate with C/EBPα. However, all deletions that removed amino acids between positions 151 and 272 totally abolished the in vitro interaction of RTA with C/EBPα (Fig. 9C).

To further characterize the region between positions 151 and 272 that interacted with C/EBPα, a number of site-specific amino acid substitutions were introduced into the N-terminal basic segment of that region (Fig. 10A). Using as a parent the deletion protein RTA(151–548), paired Lys or Arg basic residues K152 and K154, R160 and R161, or R166 and R167 were targeted for mutation to Glu or Gly. The ability of all three K152/K154, R160/R161, and R166/R167 mutants to interact with GST-C/EBPα was significantly impaired compared to that of wild-type RTA(151–548). Double mutations of the above sites, as in mutants RTA(151–548KR1), RTA(151–548KR2), and RTA(151–548RR), led to an even lower affinity for GST-C/EBPα; the triple mutation of the above sites, as in mutant RTA(151–548KRR), completely abolished the interaction with

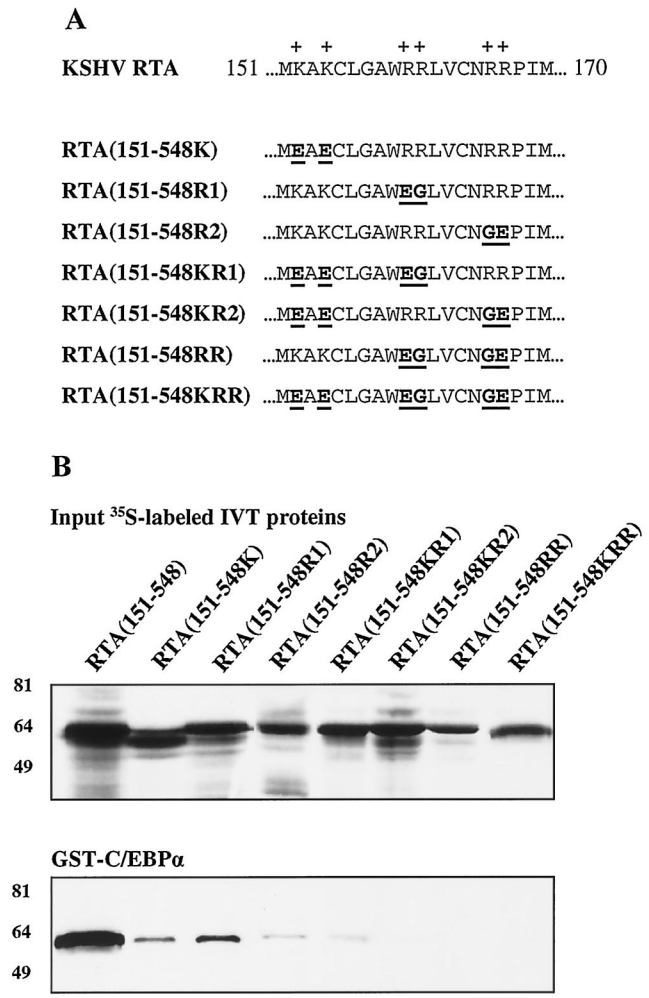

FIG. 10. Basic amino acid residues mapping between amino acids 151 and 170 of RTA are required for interaction with C/EBPα. (A) Schematic showing the amino acid sequences of positions 151 to 170 of RTA and the seven site-specific RTA mutant versions of RTA(151–548) that harbor specific mutations of basic residues. Underlining and bold type indicate mutations. (B) (Upper panel) Relative sizes and abundances of the ^{35}S-labeled in vitro-translated (IVT) RTA mutants synthesized in vitro. (Lower panel) Results of in vitro GST affinity binding assays showing the relative levels of the different RTA mutants that were recovered after binding to purified GST-C/EBPα fusion beads. Numbers at left indicate mass in kilodaltons.

GST-C/EBPα (Fig. 10B). Therefore, the six basic amino acids at positions 152, 154, 160, 161, 166, and 167 (at the end of the N-terminal basic domain) are crucial for the ability of RTA to interact with C/EBPα.

An N-terminal domain of KSHV RTA upstream of position 112 is required for both DNA binding and dimerization. To attempt to characterize the DBD of RTA, in vitro-translated truncation and deletion mutants RTA(1–377), RTA(1–377Δ11–112), and RTA(151–548) were used in EMSAs with probe PAN-RRE. Truncated RTA(1–377) bound to probe PAN-RRE in these assays with a much higher affinity than did full-length RTA (Fig. 11A, lanes 2 and 4) and formed a single shifted band at a faster-migrating position relative to the wild-type RTA band shift. In contrast to intact RTA, the complex could not be supershifted by our RTA rabbit antiserum, which recognizes an epitope between positions 527 and 539 of RTA (Fig. 11A, lanes 3 and 5). However, RTA(1–377Δ11–112) was unable to bind to probe PAN-RRE at all, suggesting that the region from positions 11 to 112 was needed for the DNA binding activity of RTA. Furthermore, both RTA(151–548) (Fig. 11A, lane 12) and RTA(1–273) (data not shown), which both still interacted with C/EBPα, were unable to bind to probe PAN-RRE; however, because of the relatively low abundance of the latter protein fragment, weak DNA binding could not be excluded.

When both full-length RTA and RTA(1–377) were cotranslated together in vitro, an additional novel intermediate heterodimeric form was able to form a complex with probe PAN-RRE; the addition of RTA antibody apparently led to the formation of two supershifted bands, one at a corresponding intermediate position and one for full-length RTA (Fig. 11A, lanes 6 and 7). However, only the full-length RTA shifted band was observed when wild-type RTA and RTA(1–377Δ11–112) or wild-type RTA and RTA(151–548) were cotranslated together (Fig. 11A, lanes 8 to 15). These results implied that an N-terminal domain from positions 1 to 151 of RTA, including a segment between positions 11 and 112, was required for DNA binding and that a dimerization domain mapping within the N-terminal 377 amino acids of the protein also required a segment between positions 11 and 112.

Finally, we also examined whether the RTA(1–377) domain that bound very efficiently to probe PAN-RRE could also bind to probe RAP-RRE. However, just like intact RTA(1–691) (Fig. 11B, lane 4), it completely failed to do so (Fig. 11B, lane 5). Parallel positive control lanes showed efficient and specific C/EBPα binding to the same probe (Fig. 11B, lanes 2 and 3). Therefore, despite the strong binding of in vitro-translated RTA(1–691) and RTA(1–377) to probe PAN-RRE, we were unable to detect any evidence for direct binding to probe RAP-RRE in vitro.

An RTA deletion mutant lacking the basic domain fails to interact with C/EBPα or to bind to DNA. Site-specific substitution analysis showed that several basic residues present within the region from amino acids 151 to 170 in RTA are required for the interaction of RTA with C/EBPα. Therefore, the entire basic region between amino acids 151 and 167 was deleted to generate an RTA(Δ151–167) mutant expression vector driven by the HCMV enhancer-promoter. As expected, the 110-kDa version of [^{35}S]methionine-labeled in vitro-translated RTA failed to bind to the GST-C/EBPα fusion at all in a GST affinity column (Fig. 12A). However, because the deleted region was very close to the RTA DBD, we wished to further investigate whether this region might also be required for RTA to bind to known DNA target sequences, such as the type II RRE in the PAN promoter. EMSA analysis performed with in vitro-translated RTA(Δ151–167) and probe PAN-RRE confirmed that RTA(Δ151–167) also had lost the ability to bind to DNA (Fig. 12B).

We further investigated whether this RTA mutant might still retain any transactivation abilities that might be mediated through some unknown mechanism independent of either C/EBPα-mediated interactions or type II RRE DNA binding. However, LUC reporter gene assays done with three different reporter gene plasmids showed that the RTA(Δ151–167) mu-

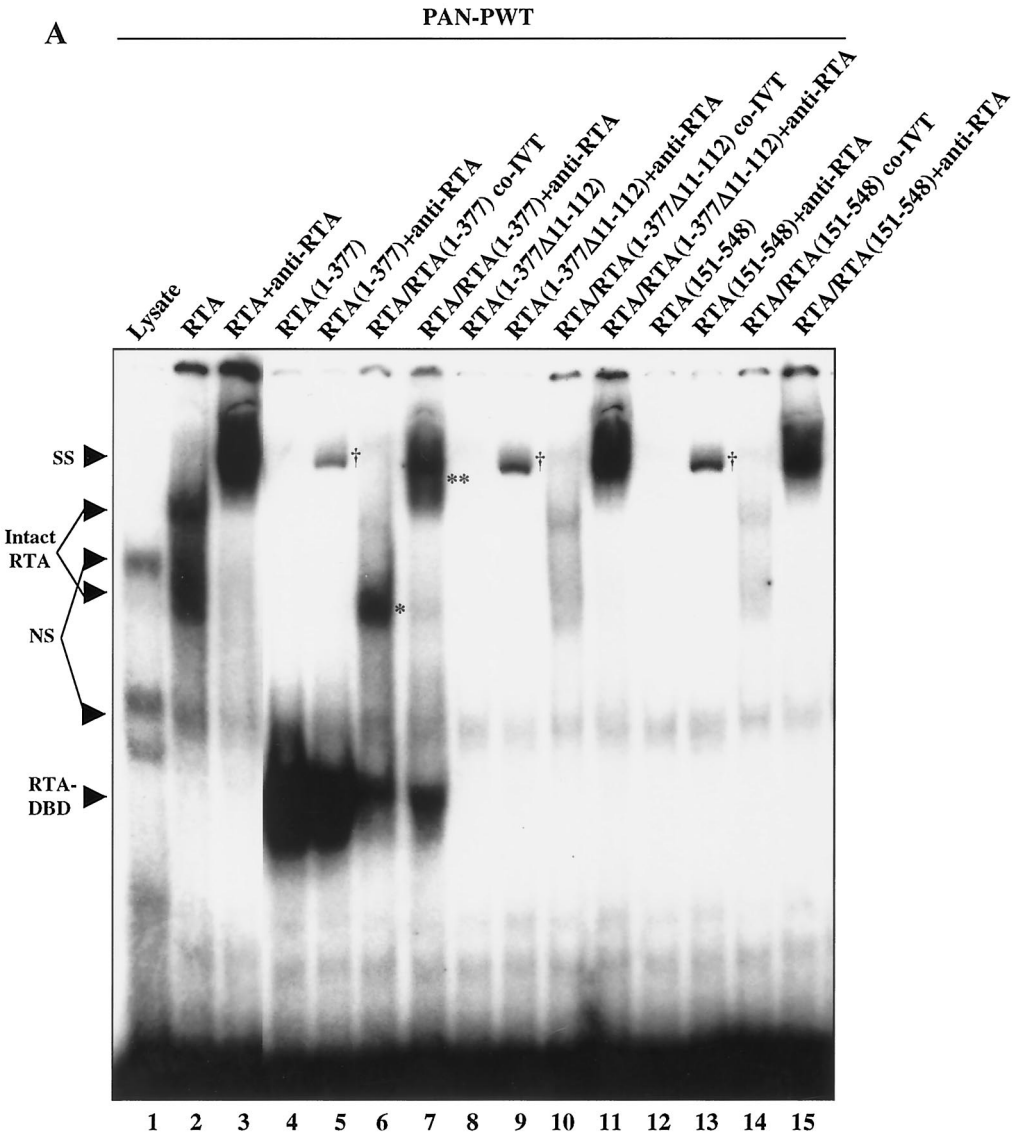

FIG. 11. Evaluation of the specific DNA binding affinities and dimerization of RTA C-terminal and N-terminal domain deletion mutants. (A) ^{32}P-labeled probe PAN-RRE was used to test the binding activities of three RTA deletion mutants in EMSA experiments. RTA(1–377), RTA(1–377Δ11–112), and RTA(151–548) were singly translated or cotranslated as well as incubated with specific rabbit polyclonal anti-RTA serum. Both DNA binding activity and heterodimerization were abolished by deletion of amino acids from positions 1 to 151 or from positions 11 to 112. Asterisk, heterodimer. Double asterisk, antibody-supershifted heterodimer. Dagger, nonspecific DNA binding activity present in undiluted rabbit antiserum. IVT, in vitro translated; SS, supershifts; NS, nonspecific shifts. (B) Lack of binding by RTA(1–377) to ^{32}P-labeled probe RAP-RRE. Parallel EMSA experiments were carried out with in vitro-translated C/EBPα (lanes 2 and 3), RTA(1–691) (lane 4), and RTA(1–377) (lane 5). Lane 3 shows supershifting with anti-C/EBPα antiserum. S, shifts.

tant was completely inactive in transcriptional assays. Not only did RTA(Δ151–167) fail to activate the $(RAP\text{-}C/EBP\text{-}II)_3$-A10-LUC and wild-type RAP promoter-LUC reporter genes, but also it failed to activate the PAN promoter-LUC reporter gene (Fig. 12C). In addition, the cooperativity observed between full-length RTA and C/EBPα was not observed at all with the RTA(Δ151–167) mutant (Fig. 12C). These results confirmed that RTA transactivation required the basic domain between amino acids 151 and 167, which binds C/EBPα; unfortunately, however, because DNA binding activity was lost, this mutant did not permit discrimination between the two alternative mechanisms of RTA transactivation described here: direct DNA binding and C/EBPα-mediated interactions.

RAP also modulates transactivation of the RAP promoter by C/EBPα and RTA. In EBV, ZTA is able to both positively and negatively autoregulate its own promoter during the lytic cycle (14, 21, 22). Although RAP is not known to bind directly to DNA and certainly does not bind to ZTA response element (ZRE) or AP-1 sites, it can still activate both the C/EBPα promoter and the p21 promoter through interactions with C/EBPα (49; Wu et al., unpublished). Since KSHV RAP is distantly related to EBV ZTA, we wished to investigate

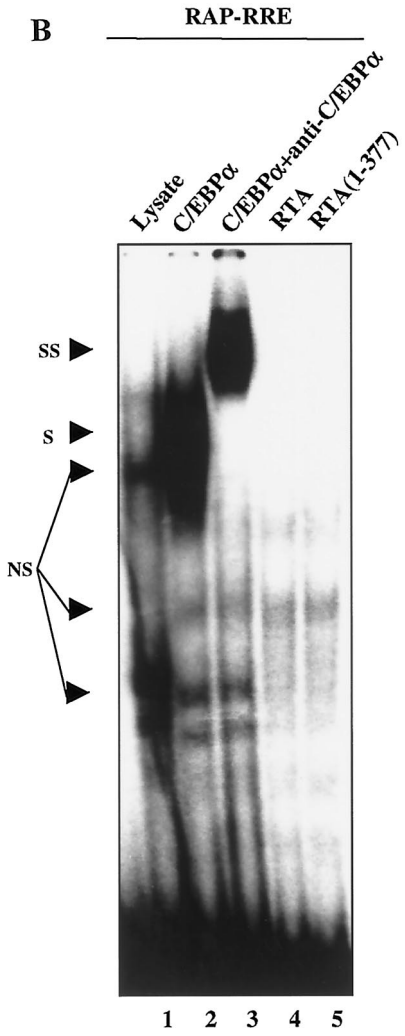

FIG. 11—*Continued*.

whether RAP might autoregulate its own promoter, perhaps indirectly through C/EBPα and RTA. Therefore, the target RAP promoter-LUC reporter gene was cotransfected into Vero cells together with the C/EBPα, RAP, and RTA expression plasmids either alone or in combination (Fig. 13A).

Although RAP by itself did not upregulate its own promoter (0.9-fold effect), it more than doubled transactivation by C/EBPα from 42- to 93-fold; this enhancement was further heightened by increasing the amount of RAP in the presence of a constant C/EBPα level, leading to a maximum activation of the RAP promoter that reached 120-fold (Fig. 13A). In addition, RAP was also able to moderately enhance the effect of RTA on the RAP promoter from 15- to 35-fold (Fig. 13A). Again, the combination of C/EBPα and RTA together increased their activation effect from 42- and 15-fold, respectively, up to 155-fold. Finally, the triple combination of RAP with both C/EBPα and RTA led to an additional effect that enhanced transactivation from 155-fold (without RAP) to 260-fold (with RAP) (Fig. 13A).

Direct interaction between RTA and RAP. It was recently found that RAP interacts strongly with C/EBPα in vitro and in coimmunoprecipitation assays with infected or transfected cells, as well as cooperatively enhancing C/EBPα-mediated transcriptional activation of the C/EBPα and p21 promoters in reporter gene assays (49; Wu et al., unpublished). Because we also observed cooperativity between RAP and RTA here even in the absence of cotransfected C/EBPα, we examined whether the two KSHV early lytic-cycle proteins might in fact interact with each other. An immunoprecipitation experiment was performed with in vitro-translated Myc-tagged RAP and target untagged RTA, both of which were [^{35}S]methionine labeled. A mixture of an anti-Myc MAb and protein A-protein G–Sepharose beads was used to immunoprecipate Myc-RAP. After thorough washing of the beads, we were able to detect coimmunoprecipitated RAP (Fig. 13B, lane 5). As positive controls, we were able to detect coimmunoprecipitation of both Myc-RTA and Myc-RAP with untagged C/EBPα (Fig. 13B, lanes 2 and 4); as negative controls, we were unable to detect immunoprecipitation of untagged C/EBPα or untagged RTA with the anti-Myc MAb (Fig. 13B, lanes 6 and 7).

To further evalute the interaction between RTA and RAP, we performed GST affinity assays with wild-type GST-RTA or the GST-RTA(1–377) fusion and ^{35}S-labeled in vitro-translated RAP. Amino acids 1 to 377 of RTA were previously described to encompass the RTA DBD. We were able to recover ^{35}S-labeled RAP from thoroughly washed Sepharose beads fused to GST-RTA and the GST-RTA(1–377) fusion, although RAP interacted relatively weakly with the GST-RTA(1–377) fusion compared to a two- to threefold stronger interaction with intact GST-RTA (Fig. 13C). Therefore, the coimmunoprecipitation of RTA by Myc-RAP, as well as the recovery of ^{35}S-labeled RAP from the GST-RTA fusion attached to beads, indicated that a direct interaction could occur in vitro between RAP and RTA.

Finally, the in vivo interaction between RTA and RAP was confirmed by an endogenous coimmunoprecipitation assay with nuclear extracts from TPA-treated BCBL-1 cells (Fig. 13D). We were able to efficiently recover the 120-kDa RTA band from an immunoprecipitate with an anti-RAP PAb (Fig. 13D, lane 3). For comparison, the RTA bands from the input BCBL-1 cell nuclear extract were detected directly by Western immunoblotting (Fig. 13D, lane 1). As a positive control, the RTA band was also immunoprecipitated with the anti-RTA PAb (Fig. 13D, lane 2); a negative control was performed with preimmune rabbit serum, which failed to recover any RTA (Fig. 13D, lane 4). These results suggested that the coimmunoprecipitation experiment was highly specific.

DISCUSSION

During the early stages of KSHV lytic-cycle induction, RAP (K8) is induced from an inactive latent-state basal level to a very high level within 12 to 48 h (24, 32, 49, 52), and we have inferred that there is a crucial need for high levels of RAP during the early stages of the KSHV lytic cycle. The function of RAP initially remained obscure in spite of early optimism that it might behave in a fashion similar to that of a positionally and evolutionarily related but nonhomologous analogue, ZTA, which triggers the full lytic-cycle cascade of EBV. However,

unlike ZTA, RAP proved unable to either trigger the full KSHV lytic-cycle process or transcriptionally induce a number of expected downstream KSHV promoter targets. Furthermore, RAP failed to bind directly to the known ZRE- and AP-1-like DNA motifs that ZTA binds to efficiently (C.-J. Chiou, F. Wu, and G. S. Hayward, unpublished data). Among the important aspects of EBV ZTA are the facts that it can autoregulate its own promoter and maintain a high level of expression throughout the lytic cycle, even when its initial upstream cellular or viral triggers cease to exist or function. ZTA achieves this transactivation of its own promoter through direct binding to two ZRE binding sites (ZIIIA and ZIIIB) found in the proximal upstream ZTA promoter (9, 12, 14, 21, 22, 28). We found that, unlike ZTA, RAP neither bound to its own promoter directly nor resulted in any transactivation of a target RAP promoter-LUC reporter gene when transfected alone (45).

However, recent studies suggested that RAP, despite its inability to bind directly to DNA, is nevertheless still functionally homologous to ZTA in several ways. For example, RAP is actively involved in the process of viral DNA replication. RAP not only is found in the viral DNA replication compartments but also is targeted to the PODs (or ND10), where viral DNA replication seems to initiate. In addition, RAP also facilitates the nuclear transport of KSHV primase-associated factor, a critical member of the six protein components of the KSHV core replication machinery (50). Most recently, it was found that RAP is able to arrest the host cell cycle at G_1 to facilitate the progression of viral replication and that this process is mediated through the induction of cellular C/EBPα and p21, both potent inhibitors of G_1/S cell cycle progression (49; Wu et al., unpublished). C/EBPα was the first DNA binding transcriptional activator identified with a leucine zipper motif (bZIP) (19). In addition to the fact that RAP interacts physically with C/EBPα (Chiou et al., unpublished), the recent discovery that ZTA, also a member of the bZIP family, interacts with C/EBPα to mediate G_1/S cell cycle arrest (50a) suggested that C/EBPα plays a very important role in the lytic cycle of all gamma-class herpesviruses.

Although KSHV RTA was already implicated as the main viral trigger that transactivates both the RAP promoter and the full lytic cycle (25, 45), we expected that cellular factors were also likely to contribute to RAP induction, partly because cellular factors are involved in ZTA promoter responses. RAP expression is triggered as early as 12 h after the onset of the lytic cycle (24, 52), and during these early stages, the amount of RTA may not reach a level sufficient to fully activate RAP expression and facilitate viral DNA replication. Conceivably, cellular factors are needed to cooperatively boost the initial thrust of RAP expression either with or without RTA. Although other candidate cellular proteins, such as NF-κB, GATA-1, and octamer binding protein 2 (OCT-2), have been reported to have putative binding sites within the RAP promoter (25, 45), we suspected that C/EBPα may play a role in activating the RAP promoter, because the levels of C/EBPα were strongly induced in PEL cells during the early lytic cycle. Furthermore, we had learned that C/EBPα expression was mediated by increased levels of RAP and not by TPA treatment itself and that RAP could cooperate with C/EBPα to transactivate the C/EBPα promoter (49; Wu et al., unpublished).

The identification of a strong C/EBPα binding site in the RAP promoter suggested that RAP might in fact indirectly influence its own expression also through the induction of C/EBPα. Functional data presented in this study proved that C/EBPα indeed is able to activate the RAP promoter through direct binding to the C/EBP binding site. Therefore, RAP can induce C/EBPα, and C/EBPα can in turn further consolidate and enhance the expression of RAP, contributing to a powerful interdependent positive regulatory mechanism that boosts the expression of both proteins.

Among the most important discoveries from this study are that C/EBPα physically interacts with RTA and that the combination of RTA, C/EBPα, and RAP can cooperatively elevate the transactivation of RAP from minimal basal levels to over 250-fold, more than 8- and 16-fold higher, respectively, than the levels obtained with the same doses of either C/EBPα or RTA alone. These results are consistent with our IFA data indicating that the introduction of either exogenous RTA or C/EBPα alone contributed to RAP activation in 82 and 74% of transfected BCBL-1 cells, respectively, whereas cotransfection of both RTA and C/EBPα led to RAP activation in 98% of RTA-positive transfected cells. Furthermore, the high levels of induction of the RAP promoter-LUC reporter gene observed in transient reporter assays with RTA plus C/EBPα are consistent with the rapid elevation of RAP expression detected by Western immunoblotting (49).

Contrary to our previous assumption that RAP does not act on its own promoter at all, our current data suggest that RAP in fact plays an indirect but significant role in activating its own promoter, primarily through an interaction with RAP promoter-bound C/EBPα. Therefore, the final consequence of this mechanism is somewhat similar to ZTA autoregulation in EBV, although RAP does not bind to RAP promoter DNA directly but instead via C/EBPα, as shown by our ChIP assays, and RAP cannot function in the absence of C/EBPα, as shown by our LUC cotransfection assays. Our additional finding that RAP also interacts with KSHV RTA seems to suggest that the cooperative interactions among all three proteins, i.e., RAP, C/EBPα, and RTA, probably correspond to the highest levels of RAP mRNA and RAP expression. Despite the similar cooperative autoregulation, the question of whether EBV RTA interacts directly with ZTA does not appear to have been addressed in the literature. The observed lack of ability of RAP alone to activate expression from its own promoter either directly or indirectly in our cotransfection experiments probably implies either that endogenous C/EBPα levels are too low in all of the cell types tested, as well as in uninduced PEL cells, or that other, related but counteracting proteins in this pathway, such as C/EBPβ or CHOP-10, are more abundant.

Lukac et al. reported that baculovirus-derived KSHV RTA binds directly to the 16-bp RRE sequence on the RAP (K8) promoter (25), and our ChIP assay results suggested that some RTA does indeed bind either to the RAP RRE or elsewhere in the RAP promoter in lytically infected cells in the absence of C/EBPα, although at a much lower efficiency than when C/EBPα is present. However, we also observed (i) that even the 49-bp probe RAP-RRE had an affinity in vitro for RTA several orders of magnitude lower than did probe PAN-RRE

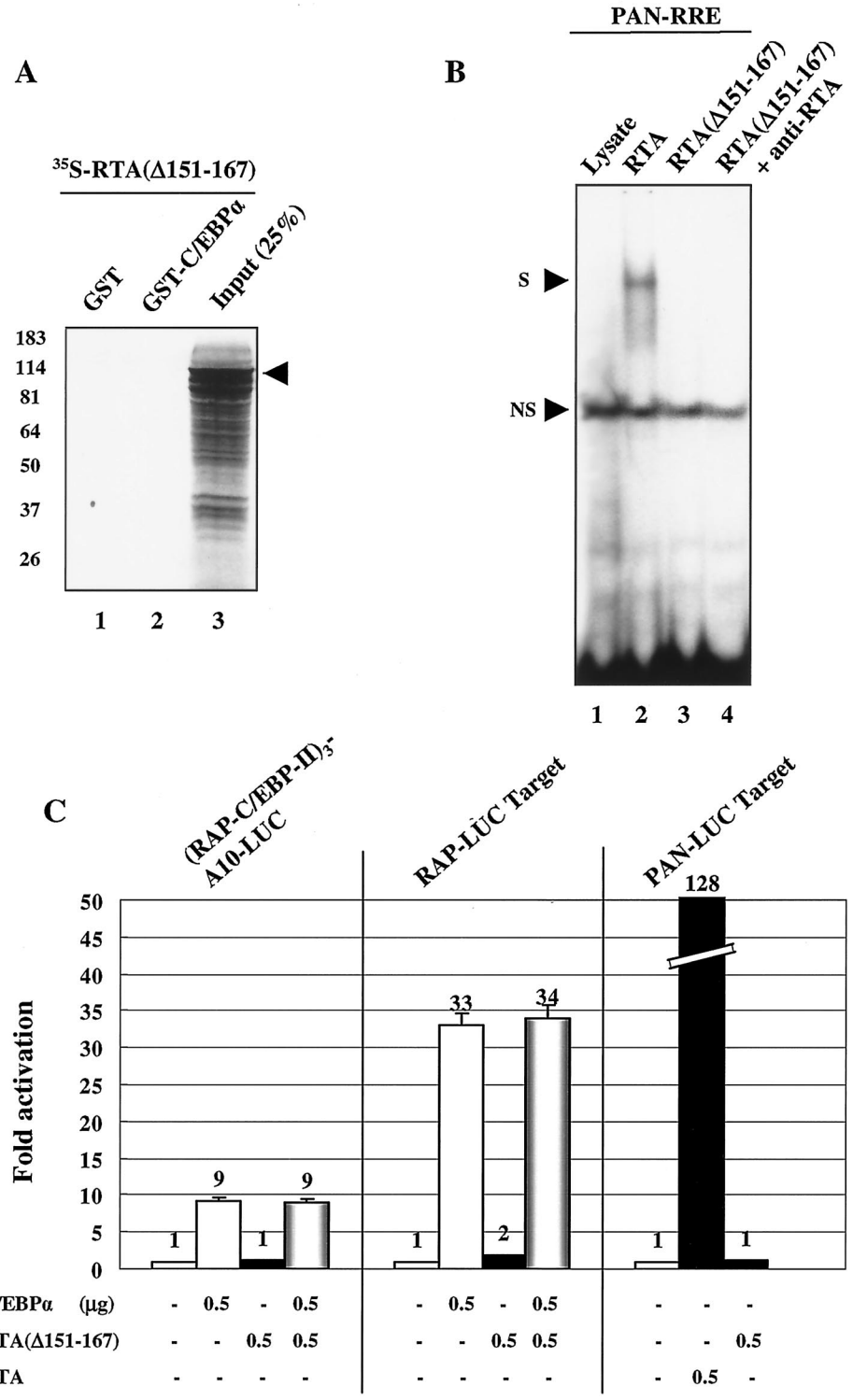

FIG. 12. The RTA(Δ151–167) deletion mutant fails to interact with C/EBPα, to bind RRE DNA, to cooperate with C/EBPα, or to transactivate RRE containing target promoters. (A) GST affinity assay showing the absence of an interaction between GST-C/EBPα and ^{35}S-labeled RTA(Δ151–167). Lanes 1 and 2, lack of RTA(Δ151–167) binding to either GST or a GST-C/EBPα fusion. Lane 3, control showing input in vitro-translated ^{35}S-labeled RTA(Δ151–167). Numbers at left indicate mass in kilodaltons. (B) EMSA showing the absence of binding of in vitro-translated RTA(Δ151–167) to probe PAN-RRE. Lane 1, reticulocyte lysate used as a negative control; lane 2, positive control showing in vitro-translated full-length RTA; lane 3, in vitro-translated RTA(Δ151–167); lane 4, in vitro-translated RTA(Δ151–167) plus anti-RTA PAb. S, shifts; NS, nonspecific shifts. (C) Histograms comparing the results of transient LUC reporter assays in which the target (RAP-C/EBP-II)$_3$-A10-LUC reporter, RAP promoter-LUC reporter, and PAN promoter-LUC reporter genes were transiently expressed in HeLa cells either alone or in the presence of mammalian expression plasmids encoding full-length C/EBPα, RTA(Δ151–167), a combination of both C/EBPα and RTA(Δ151–167), or full-length RTA as a positive control.

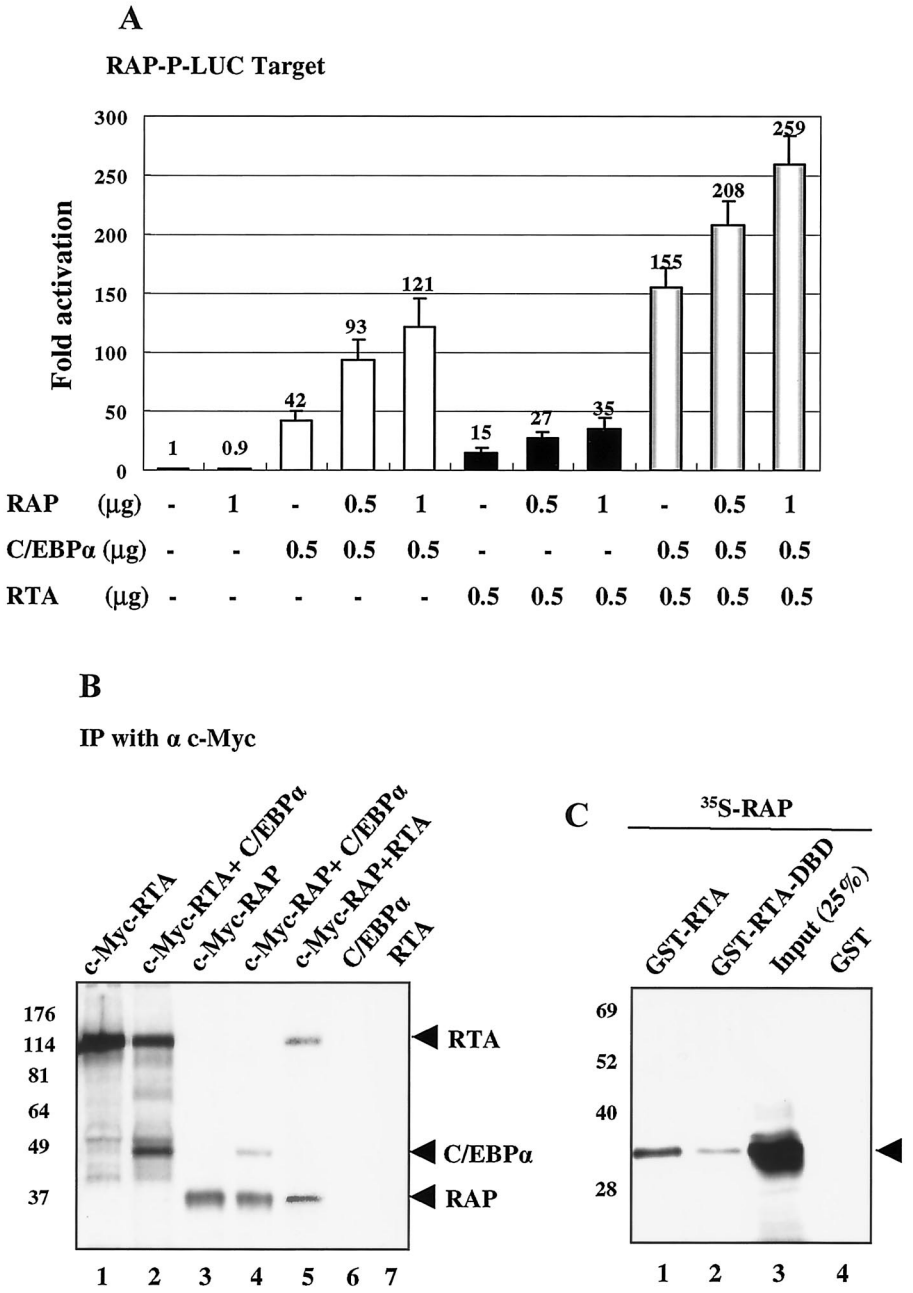

FIG. 13. KSHV RAP interacts directly with both RTA and C/EBPα and enhances their transactivation of the KSHV RAP (K8) promoter. (A) Histogram showing the results of dose-response transient LUC reporter assays in which the target wild-type RAP(−190/+10)-LUC reporter gene was transfected into Vero cells either alone or in the presence of various combinations of mammalian expression plasmids encoding C/EBPα, RTA, and RAP. (B) Coimmunoprecipitation assays showing in vitro interactions between ^{35}S-labeled in vitro-translated C/EBPα, RTA, and RAP. Experiments were performed by immunoprecipitation (IP) of Myc-tagged proteins with anti-Myc MAb and detection of bound untagged target ^{35}S-labeled proteins in the immunoprecipitates. Lane 1, in vitro-translated Myc-RTA only, in a direct positive control immunoprecipitation with anti-Myc MAb. Lane 2, mixture of in vitro-translated Myc-RTA and untagged C/EBPα, showing recovery of both after immunoprecipitation with anti-Myc MAb. Lane 3, in vitro-translated Myc-RAP only, in a direct immunoprecipitation of Myc-RAP alone with anti-Myc MAb. Lane 4, mixture of in vitro-translated Myc-RAP and untagged C/EBPα, showing recovery of both after immunoprecipitation with anti-Myc MAb. Lane 5, mixture of in vitro-translated Myc-RAP and untagged RTA, showing recovery of both after immunoprecipitation with anti-Myc MAb. Lanes 6 and 7, negative controls showing that ^{35}S-labeled untagged C/EBPα and RTA could not be immunoprecipitated directly with anti-Myc MAb. (C) In vitro GST affinity assays showing an interaction between RTA and RAP. Lanes 1 and 2, recovery of ^{35}S-labeled in vitro-translated RAP bound to GST-RTA or to a GST-RTA(1–377) fusion. Lane 3, input in vitro-translated ^{35}S-labeled RAP. Lane 4, negative control showing that GST alone failed to bind to ^{35}S-labeled RAP. (D) Coimmunoprecipitation of KSHV RTA with RAP from nuclear extracts (NE) of KSHV-positive BCBL-1 cells at 30 h after lytic-cycle induction by TPA. Detection was carried out by Western immunoblotting with anti-RTA PAb. Lane 1, positive control showing RTA in the BCBL-1 cell nuclear extract (10 μl, 10% of input sample). Lane 2, positive control showing recovery of RTA by immunoprecipitation with anti-RTA PAb. Lane 3, recovery of RTA after immunoprecipitation with anti-RAP PAb. Lane 4, negative control showing that immunoprecipitation with control preimmune rabbit serum failed to recover any RTA. Arrowheads indicate reactive bands, and numbers at left indicate mass in kilodaltons.

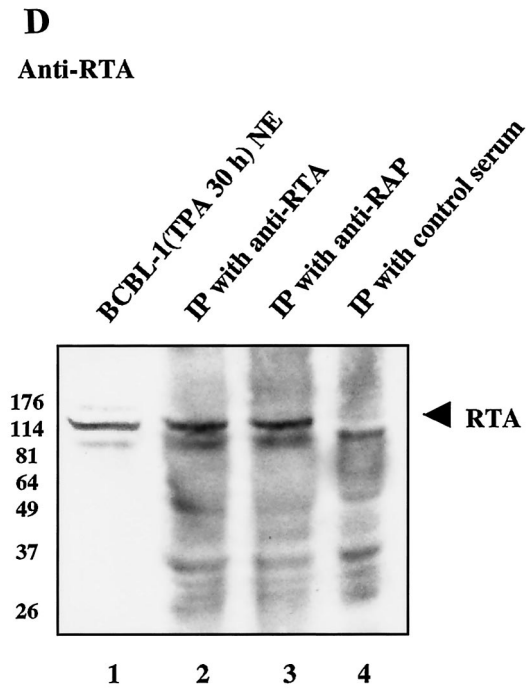

FIG. 13—*Continued*.

and an affinity for C/EBPα several orders of magnitude higher and (ii) that the addition of RTA to the C/EBPα-bound probe RAP-RRE DNA caused a dose-dependent loss of the shifted band in EMSA experiments. We believe that supercomplexes containing both C/EBPα and RTA (or C/EBPα and RAP) bound to DNA may not be formed stably in vitro in EMSA experiments because they either are too large or require distortions of the DNA helix. However, our in vivo ChIP assay results do suggest that without C/EBPα, the amount of RTA bound to DNA is greatly reduced, although not as much as for RAP, where association with the RAP promoter is abolished in the absence of C/EBPα.

RTA clearly binds strongly in vitro to some RRE motifs (such as the PAN type II RRE motif) on its own independently of C/EBPα. Lukac et al. (25) also showed that both baculovirus-expressed full-length RTA and an *E. coli*-derived RTA(1–273) fragment produced shifted bands for the mRNA transport and accumulation protein (MTA, or ORF57) promoter type I RRE motif, which closely resembles the RAP type I RRE motif. However, the situation is not entirely clear for the RAP type I RRE motif. Our studies showed that neither full-length RTA(1–691) nor the RTA(1–377) fragment produced by in vitro translation bound at all to the RAP RRE in EMSA experiments. However, both bound efficiently to the PAN type II RRE motif. These results imply either that C/EBPα or some other cellular protein mediates the binding of RTA to the RAP RRE in vivo or that forms of RTA with different posttranslational modifications have different affinities for the two types of RREs.

In addition, RTA seems capable of transactivating heterologous promoters containing a variety of core or consensus C/EBP binding sites in the absence of the complete RAP RRE. This finding suggests that the RTA-mediated enhancement of C/EBPα transactivation may be a more global phenomenon rather than that it occurs just in this special case involving the KSHV RAP promoter. Because of the inability of RTA to bind directly to C/EBP binding sites (including the overlapping RAP RRE and C/EBP-II binding site), it is reasonable to assume that RTA may mediate the transactivation of many promoters containing consensus C/EBP binding sites through a piggyback mechanism, with RTA binding being mediated by DNA-bound C/EBPα. One important piece of evidence supporting this model comes from the transient reporter cotransfection assay performed with the target $(C/EBP\text{-}II)_3$-A10-LUC reporter gene, which contains only the core C/EBP-II motif and not the rest of the previously defined RAP RRE sequence (AATGATT). Because we were unable to observe any direct RTA binding to even wild-type probe RAP-RRE, the DNA sequence in $(C/EBP\text{-}II)_3$-A10-LUC almost certainly fails to mediate direct RTA binding to the RAP promoter in vivo. Even Lukac et al. (25) showed in their system that the absence of AATGATT completely destroys the ability of RTA to bind to the RAP promoter directly. Nevertheless, RTA could still activate our C/EBP motif reporter gene sevenfold. However, when the RTA(Δ151–167) mutant, which is unable to interact with C/EBPα at all, was used, the transactivation of this and all other tested reporter genes was completely abolished. These results suggested that the interaction with C/EBPα is crucial for RTA-mediated activation of this heterologus reporter gene even in the absence of the complete RRE. Further, since C/EBPα can autoregulate its own promoter, RTA may potentially enhance this process, leading to further elevated C/EBPα expression. Additional studies are needed to confirm the notion that KSHV RTA, like RAP, is able to induce C/EBPα expression from an existing basal level.

Nevertheless, RTA transactivation of the C/EBP binding site-containing heterologous promoter was much weaker than that of the KSHV RAP promoter. Therefore, the strong activation by RTA of the RAP promoter may be attributed to the unique juxtaposition of a C/EBP binding site (AAACAAT) next to an RTA-specific recognition component of the RRE (AATGATT), to which RTA may be able to bind only in the context of DNA-bound C/EBPα. This motif would resemble the overlapping OCT and TAATGARAT motifs in herpes simplex virus immediate-early promoters, in which these motifs act as functional response elements for herpes simplex virus VP16 only when it is piggybacked on the DNA-bound OCT-1 protein. Overall, our data strongly suggest that RTA and C/EBPα interact with each other in vivo and that the two proteins probably cooperatively bind to the RRE region of the KSHV RAP promoter to maximize the level of transactivation.

In summary, we propose the following model for the activation of the RAP promoter. First, C/EBPα stably binds to the core AAACAAT motif in the crucial C/EBP-II binding site; then, RTA itself physically interacts with C/EBP-II motif-bound C/EBPα, but with part of its DBD also interacting secondarily with the adjacent RRE-specific DNA sequence AATGATT. Perhaps another C/EBPα dimer also further stabilizes the C/EBPα-RTA complex through binding to the additional adjacent weak C/EBP-I binding site upstream of the RRE and forming a bridge to the second subunit of the RTA dimer. Once a heightened level of RAP expression is estab-

lished, mediated by C/EBPα or C/EBPα plus RTA, RAP then appears capable of further positively autoregulating itself by interacting with either or both DNA-bound C/EBPα and RTA to form a tripartite RAP-C/EBPα-RTA supercomplex.

ACKNOWLEDGMENTS

Shizhen Emily Wang and Frederick Y. Wu contributed equally to this study.

These studies were funded by National Cancer Institute research grants (RO1 CA73585 and RO1 CA81400) to G.S.H. from the National Institutes of Health. S.E.W. was a postdoctoral fellow and F.Y.W. was a graduate student in the Viral Oncology Program, Sidney Kimmel Comprehensive Cancer Center, and in the Department of Pharmacology and Molecular Sciences. F.Y.W. was also partially supported by the Anti-Cancer Drug Development Training Program (grant T32 CA09243).

We thank Honglin Chen, Gangling Liao, Yanxing Yu, and Jian Huang for providing valuable advice and technical assistance.

REFERENCES

1. **Barnes, B. J., P. A. Moore, and P. M. Pitha.** 2001. Virus-specific activation of a novel interferon regulatory factor, IRF-5, results in the induction of distinct interferon alpha genes. J. Biol. Chem. **276:**23382–23390.
2. **Calkhoven, C. F., C. Muller, and A. Leutz.** 2000. Translational control of C/EBPα and C/EBPβ isoform expression. Genes Dev. **14:**1920–1932.
3. **Cannon, J. S., D. Ciufo, A. L. Hawkins, C. A. Griffin, M. J. Borowitz, G. S. Hayward, and R. F. Ambinder.** 2000. A new primary effusion lymphoma-derived cell line yields a highly infectious Kaposi's sarcoma herpesvirus-containing supernatant. J. Virol. **74:**10187–10193.
4. **Cesarman, E., P. S. Moore, P. H. Rao, G. Inghirami, D. M. Knowles, and Y. Chang.** 1995. In vitro establishment and characterization of two acquired immunodeficiency syndrome-related lymphoma cell lines (BC-1 and BC-2) containing Kaposi's sarcoma-associated herpesvirus-like (KSHV) DNA sequences. Blood **86:**2708–2714.
5. **Cesarman, E., R. G. Nador, F. Bai, R. A. Bohenzky, J. J. Russo, P. S. Moore, Y. Chang, and D. M. Knowles.** 1996. Kaposi's sarcoma-associated herpesvirus contains G protein-coupled receptor and cyclin D homologs which are expressed in Kaposi's sarcoma and malignant lymphoma. J. Virol. **70:**8218–8223.
6. **Chang, Y., E. Cesarman, M. S. Pessin, F. Lee, J. Culpepper, D. M. Knowles, and P. S. Moore.** 1994. Identification of herpesvirus-like DNA sequences in AIDS-associated Kaposi's sarcoma. Science **266:**1865–1869.
7. **Chang, Y. N., D. L. Dong, G. S. Hayward, and S. D. Hayward.** 1990. The Epstein-Barr virus Zta transactivator: a member of the bZIP family with unique DNA-binding specificity and a dimerization domain that lacks the characteristic heptad leucine zipper motif. J. Virol. **64:**3358–3369.
8. **Chen, H., J. Lee, Y. Wang, D. Huang, R. Ambinder, and S. Hayward.** 1999. The Epstein-Barr virus latency *Bam*HI-Q promoter is positively regulated by STATs and ZTA interference with JAK/STAT activation leads to loss of BamHI-Q promoter activity. Proc. Natl. Acad. Sci. USA **96:**9339–9344.
9. **Chevallier-Greco, A., E. Manet, P. Chavrier, C. Mosnier, J. Daillie, and A. Sergeant.** 1986. Both Epstein-Barr virus (EBV)-encoded *trans*-acting factors, EB1 and EB2, are required to activate transcription from an EBV early promoter. EMBO J. **5:**3243–3249.
10. **Christy, R. J., K. H. Kaestner, D. E. Geiman, and M. D. Lane.** 1991. CCAAT/enhancer binding protein gene promoter: binding of nuclear factors during differentiation of 3T3-L1 preadipocytes. Proc. Natl. Acad. Sci. USA **88:**2593–2597.
11. **Ciufo, D. M., J. S. Cannon, L. J. Poole, F. Y. Wu, P. Murray, R. F. Ambinder, and G. S. Hayward.** 2001. Spindle cell conversion by Kaposi's sarcoma-associated herpesvirus: formation of colonies and plaques with mixed lytic and latent gene expression in infected primary dermal microvascular endothelial cell cultures. J. Virol. **75:**5614–5626.
12. **Countryman, J., and G. Miller.** 1985. Activation of expression of latent Epstein-Barr herpesvirus after gene transfer with a small cloned subfragment of heterogeneous viral DNA. Proc. Natl. Acad. Sci. USA **82:**4085–4089.
13. **Darlington, G. J., S. E. Ross, and O. A. MacDougald.** 1998. The role of C/EBP genes in adipocyte differentiation. J. Biol. Chem. **273:**30057–30060.
14. **Flemington, E., and S. H. Speck.** 1990. Autoregulation of Epstein-Barr virus putative lytic switch gene BZLF1. J. Virol. **64:**1227–1232.
15. **Flemington, E. K.** 2001. Herpesvirus lytic replication and the cell cycle: arresting new developments. J. Virol. **75:**4475–4481.
16. **Gradoville, L., J. Gerlach, E. Grogan, D. Shedd, S. Nikiforow, C. Metroka, and G. Miller.** 2000. Kaposi's sarcoma-associated herpesvirus open reading frame 50/Rta protein activates the entire viral lytic cycle in the HH-B2 primary effusion lymphoma cell line. J. Virol. **74:**6207–6212.
17. **Harris, T. E., J. H. Albrecht, M. Nakanishi, and G. J. Darlington.** 2001. CCAAT/enhancer-binding protein-alpha cooperates with p21 to inhibit cyclin-dependent kinase-2 activity and induces growth arrest independent of DNA binding. J. Biol. Chem. **276:**29200–29209.
18. **Hwang, S., Y. Gwack, H. Byun, C. Lim, and J. Choe.** 2001. The Kaposi's sarcoma-associated herpesvirus K8 protein interacts with CREB-binding protein (CBP) and represses CBP-mediated transcription. J. Virol. **75:**9509–9516.
19. **Landschulz, W. H., P. F. Johnson, and S. L. McKnight.** 1988. The leucine zipper: a hypothetical structure common to a new class of DNA binding proteins. Science **240:**1759–1764.
20. **Lane, M. D., Q. Q. Tang, and M. S. Jiang.** 1999. Role of the CCAAT enhancer binding proteins (C/EBPs) in adipocyte differentiation. Biochem. Biophys. Res. Commun. **266:**677–683.
21. **Lieberman, P. M., and A. J. Berk.** 1990. In vitro transcriptional activation, dimerization, and DNA-binding specificity of the Epstein-Barr virus Zta protein. J. Virol. **64:**2560–2568.
22. **Lieberman, P. M., J. M. Hardwick, J. Sample, G. S. Hayward, and S. D. Hayward.** 1990. The Zta transactivator involved in induction of lytic cycle gene expression in Epstein-Barr virus-infected lymphocytes binds to both AP-1 and ZRE sites in target promoter and enhancer regions. J. Virol. **64:**1143–1155.
23. **Lin, F. T., O. A. MacDougald, A. M. Diehl, and M. D. Lane.** 1993. A 30-kDa alternative translation product of the CCAAT/enhancer binding protein alpha message: transcriptional activator lacking antimitotic activity. Proc. Natl. Acad. Sci. USA **90:**9606–9610.
24. **Lin, S. F., D. R. Robinson, G. Miller, and H. J. Kung.** 1999. Kaposi's sarcoma-associated herpesvirus encodes a bZIP protein with homology to BZLF1 of Epstein-Barr virus. J. Virol. **73:**1909–1917.
25. **Lukac, D. M., L. Garibyan, J. R. Kirshner, D. Palmeri, and D. Ganem.** 2001. DNA binding by Kaposi's sarcoma-associated herpesvirus lytic switch protein is necessary for transcriptional activation of two viral delayed early promoters. J. Virol. **75:**6786–6799.
26. **Lukac, D. M., J. R. Kirshner, and D. Ganem.** 1999. Transcriptional activation by the product of open reading frame 50 of Kaposi's sarcoma-associated herpesvirus is required for lytic viral reactivation in B cells. J. Virol. **73:**9348–9361.
27. **Lukac, D. M., R. Renne, J. R. Kirshner, and D. Ganem.** 1998. Reactivation of Kaposi's sarcoma-associated herpesvirus infection from latency by expression of the ORF 50 transactivator, a homolog of the EBV R protein. Virology **252:**304–312.
28. **Miller, G.** 1990. Epstein-Barr virus, p. 1921–1958. *In* B. N. Fields and D. M. Knipe (ed.), Virology. Raven Press, New York, N.Y.
29. **Nicholas, J., V. Ruvolo, J. Zong, D. Ciufo, H. G. Guo, M. S. Reitz, and G. S. Hayward.** 1997. A single 13-kilobase divergent locus in the Kaposi sarcoma-associated herpesvirus (human herpesvirus 8) genome contains nine open reading frames that are homologous to or related to cellular proteins. J. Virol. **71:**1963–1974.
30. **Ossipow, V., P. Descombes, and U. Schibler.** 1993. CCAAT/enhancer-binding protein mRNA is translated into multiple proteins with different transcription activation potentials. Proc. Natl. Acad. Sci. USA **90:**8219–8223.
31. **Park, J., T. Seo, S. Hwang, D. Lee, Y. Gwack, and J. Choe.** 2000. The K-bZIP protein from Kaposi's sarcoma-associated herpesvirus interacts with p53 and represses its transcriptional activity. J. Virol. **74:**11977–11982.
32. **Polson, A. G., L. Huang, D. M. Lukac, J. D. Blethrow, D. O. Morgan, A. L. Burlingame, and D. Ganem.** 2001. Kaposi's sarcoma-associated herpesvirus K-bZIP protein is phosphorylated by cyclin-dependent kinases. J. Virol. **75:**3175–3184.
33. **Renne, R., W. Zhong, B. Herndier, M. McGrath, N. Abbey, D. Kedes, and D. Ganem.** 1996. Lytic growth of Kaposi's sarcoma-associated herpesvirus (human herpesvirus 8) in culture. Nat. Med. **2:**342–346.
34. **Russo, J. J., R. A. Bohenzky, M. C. Chien, J. Chen, M. Yan, D. Maddalena, J. P. Parry, D. Peruzzi, I. S. Edelman, Y. Chang, and P. S. Moore.** 1996. Nucleotide sequence of the Kaposi sarcoma-associated herpesvirus (HHV8). Proc. Natl. Acad. Sci. USA **93:**14862–14867.
35. **Slomiany, B. A., K. L. D'Arigo, M. M. Kelly, and D. T. Kurtz.** 2000. C/EBPα inhibits cell growth via direct repression of E2F-DP-mediated transcription. Mol. Cell. Biol. **20:**5986–5997.
36. **Song, M. J., X. Li, H. J. Brown, and R. Sun.** 2002. Characterization of interactions between RTA and the promoter of polyadenylated nuclear RNA in Kaposi's sarcoma-associated herpesvirus/human herpesvirus 8. J. Virol. **76:**5000–5013.
37. **Soulier, J., L. Grollet, E. Oksenhendler, P. Cacoub, D. Cazals-Hatem, P. Babinet, M. F. d'Agay, J. P. Clauvel, M. Raphael, L. Degos, et al.** 1995. Kaposi's sarcoma-associated herpesvirus-like DNA sequences in multicentric Castleman's disease. Blood **86:**1276–1280.
38. **Sun, R., S. F. Lin, K. Staskus, L. Gradoville, E. Grogan, A. Haase, and G. Miller.** 1999. Kinetics of Kaposi's sarcoma-associated herpesvirus gene expression. J. Virol. **73:**2232–2242.
39. **Tang, Q. Q., and M. D. Lane.** 1999. Activation and centromeric localization of CCAAT/enhancer-binding proteins during the mitotic clonal expansion of adipocyte differentiation. Genes Dev. **13:**2231–2241.
40. **Timchenko, N., D. R. Wilson, L. R. Taylor, S. Abdelsayed, M. Wilde, M.**

Sawadogo, and G. J. Darlington. 1995. Autoregulation of the human C/EBP alpha gene by stimulation of upstream stimulatory factor binding. Mol. Cell. Biol. **15:**1192–1202.

41. **Timchenko, N. A., T. E. Harris, M. Wilde, T. A. Bilyeu, B. L. Burgess-Beusse, M. J. Finegold, and G. J. Darlington.** 1997. CCAAT/enhancer binding protein alpha regulates p21 protein and hepatocyte proliferation in newborn mice. Mol. Cell. Biol. **17:**7353–7361.
42. **Timchenko, N. A., M. Wilde, M. Nakanishi, J. R. Smith, and G. J. Darlington.** 1996. CCAAT/enhancer-binding protein alpha (C/EBP alpha) inhibits cell proliferation through the p21 (WAF-1/CIP-1/SDI-1) protein. Genes Dev. **10:**804–815.
43. **Wan, X., H. Wang, and J. Nicholas.** 1999. Human herpesvirus 8 interleukin-6 (vIL-6) signals through gp130 but has structural and receptor-binding properties distinct from those of human IL-6. J. Virol. **73:**8268–8278.
44. **Wang, H., P. Iakova, M. Wilde, A. Welm, T. Goode, W. J. Roesler, and N. A. Timchenko.** 2001. C/EBPα arrests cell proliferation through direct inhibition of Cdk2 and Cdk4. Mol. Cell **8:**817–828.
45. **Wang, S., S. Liu, M. Wu, Y. Geng, and C. Wood.** 2001. Kaposi's sarcoma-associated herpesvirus/human herpesvirus-8 ORF50 gene product contains a potent C-terminal activation domain which activates gene expression via a specific target sequence. Arch. Virol. **146:**1415–1426.
46. **Wang, S., S. Liu, M. H. Wu, Y. Geng, and C. Wood.** 2001. Identification of a cellular protein that interacts and synergizes with the RTA (ORF50) protein of Kaposi's sarcoma-associated herpesvirus in transcriptional activation. J. Virol. **75:**11961–11973.
47. **Wang, X., E. Scott, C. L. Sawyers, and A. D. Friedman.** 1999. C/EBPalpha bypasses granulocyte colony-stimulating factor signals to rapidly induce PU.1 gene expression, stimulate granulocytic differentiation, and limit proliferation in 32D cl3 myeloblasts. Blood **94:**560–571.
48. **Whitby, D., M. R. Howard, M. Tenant-Flowers, N. S. Brink, A. Copas, C. Boshoff, T. Hatzioannou, F. E. Suggett, D. M. Aldam, A. S. Denton, et al.** 1995. Detection of Kaposi sarcoma associated herpesvirus in peripheral blood of HIV-infected individuals and progression to Kaposi's sarcoma. Lancet **346:**799–802.
49. **Wu, F., Q. Tang, H. Chen, C. ApRhys, C. Farrell, J. Chen, M. Fujimuro, M. Lane, and G. Hayward.** 2002. Lytic replication-associated protein (RAP) encoded by Kaposi's sarcoma-associated herpesvirus causes $p21^{CIP-1}$-mediated G_1 cell cycle arrest through CCAAT/enhancer-binding protein-alpha. Proc. Natl. Acad. Sci. USA **99:**10683–10688.
50. **Wu, F. Y., J. H. Ahn, D. J. Alcendor, W. J. Jang, J. Xiao, S. D. Hayward, and G. S. Hayward.** 2001. Origin-independent assembly of Kaposi's sarcoma-associated herpesvirus DNA replication compartments in transient cotransfection assays and association with the ORF-K8 protein and cellular PML. J. Virol. **75:**1487–1506.

50a. **Wu, F. Y., H. Chen, S. E. Wang, G. Liao, M. Fujimuro, C. J. Farrell, J. Huang, S. D. Hayward, and G. S. Hayward.** CCAAT/enhancer binding protein α interacts with ZTA and mediates ZTA-induced $p21^{CIP-1}$ accumulation and G_1 cell cycle arrest during the Epstein-Barr virus lytic cycle. J. Virol., in press.

51. **Zhang, D. E., P. Zhang, N. D. Wang, C. J. Hetherington, G. J. Darlington, and D. G. Tenen.** 1997. Absence of granulocyte colony-stimulating factor signaling and neutrophil development in CCAAT enhancer binding protein alpha-deficient mice. Proc. Natl. Acad. Sci. USA **94:**569–574.
52. **Zhu, F. X., T. Cusano, and Y. Yuan.** 1999. Identification of the immediate-early transcripts of Kaposi's sarcoma-associated herpesvirus. J. Virol. **73:** 5556–5567.